A THESIS FOR THE DEGREE OF DOCTOR OF PHILOSOPHY

Development of lung on a chip for mimicking particulate matter exposure conditions

Faiza Jabbar

Department of Mechatronics Engineering

GRADUATE SCHOOL

JEJU NATIONAL UNIVERSITY

2021. 02

Development of lung on a chip for mimicking particulate matter exposure conditions

Faiza Jabbar

(Supervised by Professor Kyung Hyun Choi)

A thesis submitted in partial fulfillment of the requirement for the degree of Doctor of Philosophy

2021. 02

The thesis has been examined and approved.

.....

Thesis Director: Jong-Hwan Lim, Professor, Department of Mechatronics Engineering

.....

Supervisor: Kyung Hyun Choi, Professor, Department of Mechatronics Engineering

.....

Chul Uoong Kang, Professor, Department of Mechatronics Engineering

.....

Chang-Nam Kang, Professor, Department of Mechanical Engineering

.....

Myung taek Hyun, Professor, Department of Mechanical Engineering

Date .....

Department of Mechatronics Engineering

GRADUATE SCHOOL
JEJU NATIONAL UNIVERSITY
REPUBLIC OF KOREA

Acknowledgement

In the name of ALLAH Almighty, the most Merciful and the most Beneficial. My interest in Biomedical sciences took me to the Jeju National University with the hopes of achieving a doctoral degree with practical applications in the area of research in Biomedical engineering which is fulfilled by the help of my Mentors and cooperation of Administration of the school. I admire the efforts of Professor Dr Kyung Hyun Choi for the achievement of this milestone.

Fortunately, three years journey of this degree become blissful for me to having Professor Dr. Kyung Hyun Choi as my research supervisor. I'm indebted to him for his kindness, and continuous support, planning and guidance in hard times. Positive and calm nature of the supervisor made me eligible to work in relaxed and persistent manner. I acknowledge all the efforts of my advisor and extend my gratitude to Afaque Manzoor Soomro for encouragement and welcoming attitude for guidance during the degree and in research especially.

Three years journey at JNU was not less than an adventure, with the presence of best people in my batch Afaque Manzoor Soomro, Arun Asif, Asad ullah Khalid, Abdul Rahim, Muhsin Ali and my friends Hina Ashraf, Dr Sehrish Malik, Dr wafa shafqat, Dr Irshad, Dr Gul hassan. I owe you people billons smiles and hope to see you prosperous.

I would like to give special thanks to my family parents, husband, sisters, brother for all the efforts and providing me with caring and healthy environment. I owe to prayers of my father and mother and being the best source of motivation. Irreplaceable loss of my mother during this degree shattered me, but my father's continuous help and prayers made me able to grow and persistent with my goal. I pray for your long and healthy life.

Contents

Lists of figures

Abstract

The Drug discovery process takes decades to bring a new drug to the market, preclinical animal models based drug testing results in failure of 90% drugs due to drug toxicity and inefficacy. A preclinical study of a lead compound goes through 2D cultures and animal testing to study Pharmacodynamics and pharmacokinetics for before clinical testing. Safety and efficacy of a lead compound may not be accurately predicted by utilizing these preclinical models. Preclinical phase and screening in Drug development needs more relevant models of human organ systems to avoid failures. Organ-on-chip technology is offering physiologically relevant human organ models to replace animal testing for better analysis of drugs, environmental toxins (Xenobiotics) and food testing. Organ level complexity is an obstacle to study human airway diseases and in the development of new therapeutics for Asthma and COPD. Particulate matter (PM10) induced respiratory illnesses are a challenge to study in trans-well culture system. Micro-physiological systems offer potential for mimicking these phenomena for better understanding of possible hazards to human respiratory health. Here we have developed Human Lung, Lung cancer, on a microfluidic chip equipped with a peristaltic pump, real-time microscope and system integrated pH, TEER, Dissolved Oxygen provided patho-physiologically relevant human data. The Patho-physiological significance of the human organ mimetics was well characterized by confocal laser scanning microscopy, ELISA and TEER sensor. A Highly efficient organ-on-chip device can perform high throughput drug screening analysis with accurately mimicking human physiology. The Special focus of the study was testing particulate matter (PM<10) in dynamic conditions on a microfluidic chip. Human lung distal airway models release cytokines and in large quantities, as compared to the 2D static cultures. Environmental

conditions with respect to particulate matter in air Mild 7.5*μg/ml*, Average 37.5*μg/ml* and poor 151*μg/ml* of particulate matter exposure was executed in our microfluidic system. Our study provides physiological and toxicological data of the stimulated environmental condition by inflammatory markers of respiratory disease, which leads to the identification of asthma and chronic obstructive pulmonary disease. The claims were validated by confocal microscopy and ELISA. Significant increase in IL-13, IL-6 and MUC-5AC advocated the incidence of asthma and chronic obstructive pulmonary disease conditions in our normal and cancer chips. This work will lead to the identification of potential therapeutics and prevention of chronic life-threatening toxicities. The future direction of the work is to moves towards multi-organ on a chip to study the effects of drugs on the liver and other interconnects organs for providing better clinically relevant human models

Introduction

Microfluidics, Microengineering and biomimetic principles consolidate to make physiologically relevant organ on chip systems for drug screening and disease research. Organ-on-a-chip systems have been developed for the *In vitro* toxicity evaluation in past few years. Drug discovery pipeline is imposing huge economic burden for efficacy testing and toxicity analysis. Human response to drugs varying from animal models and 2D cultures is fundamental cause of drug failure in clinical trials. Drug toxicity is the recurrent cause of prompt termination and post-market removal of drugs, leads to human and financial loss. Lack of efficient drug toxicity predicting models lead to insufficient insight into the toxic mechanism for preclinical outcomes [1]. The microenvironment of the chip simulates that of the organ in terms of tissue interfaces and mechanical stimulation by a combination of cell biology, engineering, and biomaterial technology. This reveals the structural and functional characteristics of human tissue and can predict response of drug and environmental effects to an array of stimuli. OOC has wide-ranging applications in biological diseases control application and precision. Recent breakthrough in microfluidic organ on chip technology paved the way to new insight by replacing animal models with organ on chips.

Organ-on-a-chip devices benefit from the possibility to readily include dynamic environmental factors, improving cellular fidelity, and from compatibility with imaging. Complex biological events, such as neutrophil infiltration across the vascular barrier and pulmonary leakage, can be easily visualized and quantified, enabling a detailed investigation of the mechanism of action of specific drugs or environmental insults.

This study was designed to introduce human lung-on-a-chip and lung cancer on a chip model for particulate matter exposure in dynamic fluid flow conditions, multitasking sophisticated microfluidic platform with on chip printed ITO based TEER and pH sensors equipped with in-house built microscope or real time monitoring. Glass chip of size- with top and bottom channel printed with microfabrication techniques, TEER sensor is printed on the channel directly in contact with human Lung small airway epithelial cells for continuously monitoring trans-epithelial electrical resistance after every half an hour till end of the experiment. Impedance values provide complete information of monolayer membrane integrity in control chip with flow rate of 80µl/min and shear stress of 12dyne/cm^3, four chips were introduced to our organ on chip platform for physiological and mechanically controlled growing conditions. Particulate matter exposure was introduced after four days of stable culture on chip for eight hours daily for consecutive four days with three different concentrations to mimicking routine exposure to humans in daily life. Cell monolayer consisting of Human small airway epithelial cells and co-culture of A549 lung cancer cells on other chip exhibited functions of properly differentiated epithelial cells. Airway Epithelial mucus secreting lung goblet cell and ciliated cells were confirmed by confocal microcopy. Particulate matter exposure induced inflammatory response in Human small airway cells and Co-culture of A549 and Small airway epithelial cells 12 hours showed sudden drop in impedance values correlates with cytokine secretion analysis and confocal microscopy ROS level also complements the dose dependent oxidative damage to the monolayer permeability.

Aims and objectives

This work aims at developing a biomimetic lung-on-a-chip device for drug screening. The first objective is to design a bioinspired microfluidic system based on lung biology and to study the effects of PM<10 on human lung on a chip. The long term end goal is to develop a cost effective human organs biomimetic microdevice that can be established as drug testing platform. This system must be compliant with the existing regulation for alternative methods to animal testing.

2. Particulate matter and organ on a chip

Particulate matter have become a major concern owing to their increased level in air pollution correlating with higher respiratory diseases in metropolitan cities of the world, Human health is a challenge due to rapid advancement in cities and urbanization due to emission of hazardous gases from engines of heavy vehicles and burning of fossil fuels and mining[2]. Coal burning power plants emit organic pollutants including polycyclic aromatic hydrocarbons, benzene, toluene and multitude of different gases. Weathering of soil turns clay particles into mineral dust composed of huge number of oxides and carbonates of metals. Dust storms in spring season carry the dust particles Flinches in Mongolia and Siberia moves dust particles to low-pressure areas such as eastern China, Korea, and Japan by south eastern to northwestern dust storm. Particulate matter stimulates clinical manifestations according to epidemiology and toxicology studies and contribute in developing lethal diseases such as respiratory diseases cardiovascular diseases, and mortality at an early age[3]. Human lungs are the first organ to face airborne environmental stresses such as pollutants, toxicants and pathogens as they are involved in gaseous exchange [3].

Environmental stress stimulants (particulate matter, cigarettes smoke and aerosols) are believed to be involved in the development of asthma, chronic obstructive pulmonary disease (COPD) and interstitial lung diseases [4]. Particulate matter induces release of inflammatory and allergic responsive cytokines in human airways effecting bronchiolar and alveolar passages, experimentally controlled human exposure studies suggest that interleukin-6 and tumor necrosis factor alpha (TNF-α) are key mediators of airway inflammation [5]. Allergic airways release pro-inflammatory cytokines and cause Airway hyperresponsiveness (AHR).

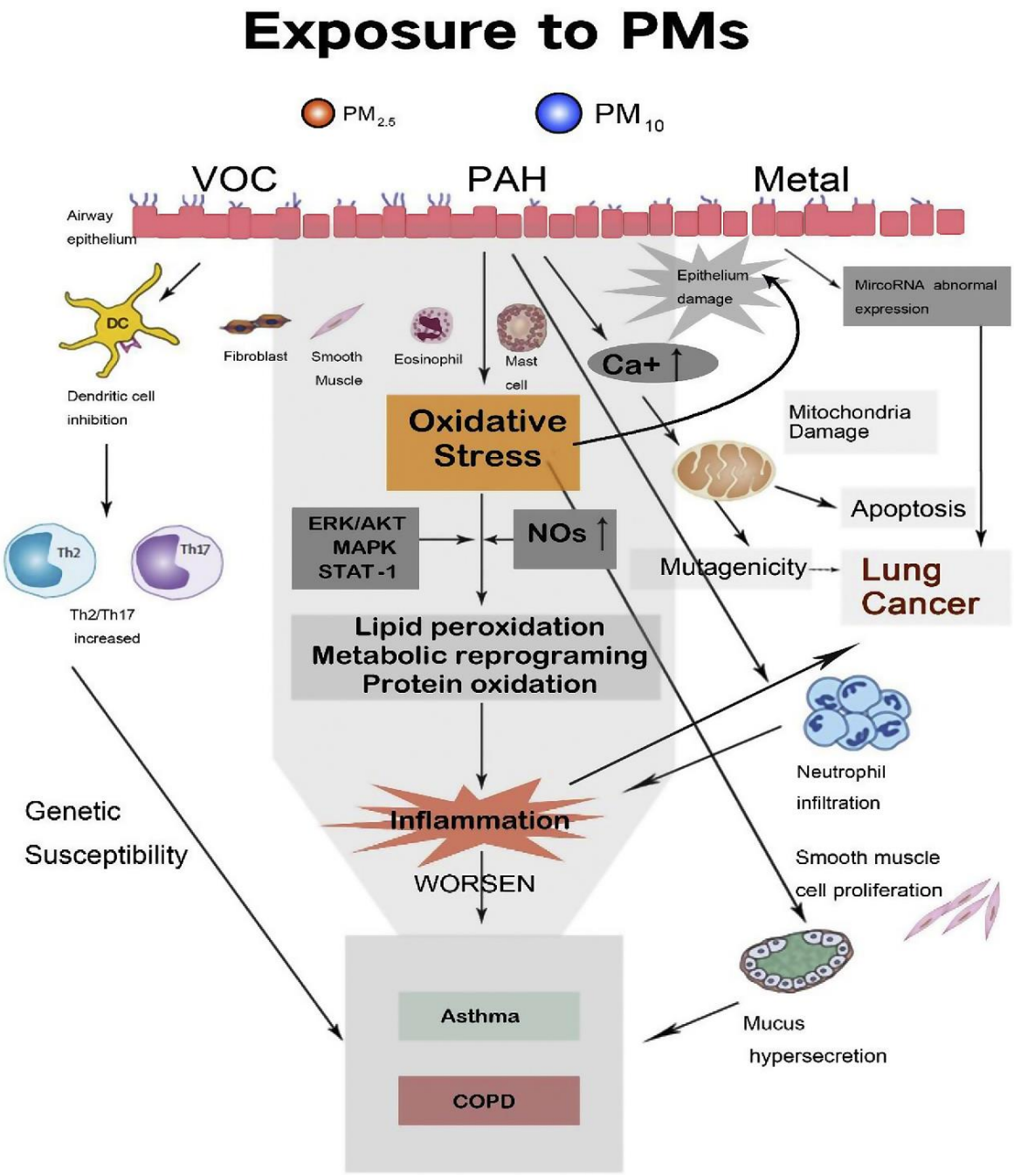

Figure 1 Mechanisms of PM's effect in allergic respiratory disease.

The immune response to allergen exposure in asthma is associated with TH2 inflammation, IL-13 is a key cytokine involved in directing allergen-induced airway inflammation and remodeling.

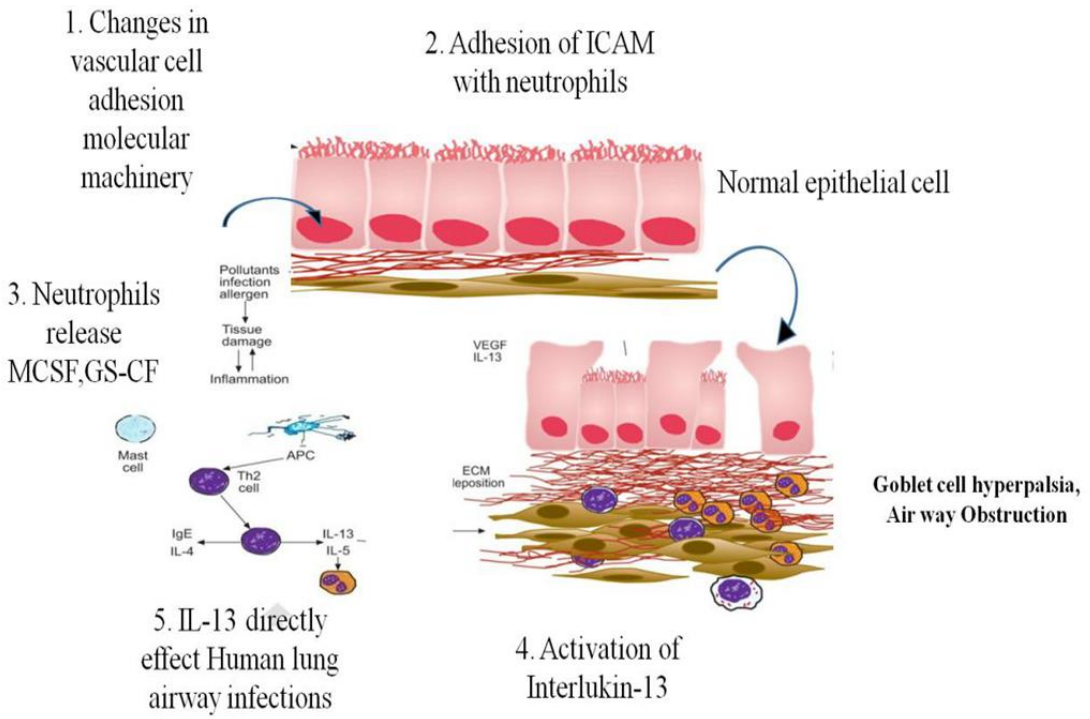

Figure 2 Mechanism of IL-13 release as incidence of asthma

In order to better understand how ambient air particulate matter (PM) affect lung health, the two main airway cell types likely to interact with inhaled particles, alveolar macrophages (AM) and airway epithelial cells have been exposed to particles in vitro and followed for endpoints of inflammation, and oxidant stress. Separation of Chapel Hill PM 10 into fine and coarse size particles revealed that the main pro-inflammatory response (TNF, IL-6, COX-2) in AM was driven by material present in the coarse PM, containing 90–95% of the stimulatory material in PM10. Regrettably animal models of asthma and allergy have failed to offer therapeutics with high efficacy, so human lung physiological mimetics are required for thorough understanding of toxicological disease analysis because animal models of inhaled toxicants and pollutants express different molecular markers from that are being produced in human subsequently resulting data usually lead to erroneous therapeutic development[6]. Animal models need to be replaced by physiologically relevant

human mimetics therefore considerable advancements have been made in development of the substitutes of organs and tissues to study such stimulation based studies. Organ on chip technology helps in revealing physiologically relevant organs by providing technologically controlled biochemical, mechanical and dynamic fluid flow conditions for recapitulating cellular microenvironment to access diseased and stressed conditions[7].

Chronic exposure to PM 10 leads to the arterial injury after residing of PM10 components in the alveolar regions of the distal airways, animals studies were conducted for arthrosclerosis in rabbit. This study to determine the effects of statins on atherogenesis and vascular function using the same rabbit model by evaluating, changes in the morphological characteristics of atherosclerotic plaques, changes in vascular endothelial function and the contribution of relevant vasoactive mediators (iNOS, COX-2, endothelin-1 (ET-1), and reactive oxygen species (ROS)]; and the expression of these vasoactive mediators in atherosclerotic lesions or systemic circulation[8]. Heavy metals transported by PM, especially in different ambient environments, exhibit different degrees of bioavailability. Bioavailability is the main controller of toxicity as it quantifes the rate at which a substance is absorbed in tissues of living systems to be physiologically available. Studies have shown that elements of human origin associated with particulate matter such as lead, chromium, nickel, zinc, copper, and cadmium are mainly mobile and have high bioavailability; these metals are adsorbed on the surfaces of PM10 particles or bonded to the particles in the form of oxides and carbonates. When in contact with a humid environment, such as in the human respiratory system where relative humidity reaches near saturation (Youn *et a*l., 2016).

Heavy metals accompanying PM10 may enter the circulatory system after being released into lung tissues. Metals may enter the cerebrospinal fluid through the circulatory

system, overcoming the blood brain barrier and passing through the plexus choroid, and transfer to a specific part of the brain (Karri et al., 2016).

The risk level of heavy metals depends on the severity of exposure and biochemical metabolism in the brain (Shahsavani *et al*., 2012) Heavy metals associated with PM10 can damage neurons and astrocytes, promoting neuropsychiatric disorders in people with exposure. Heavy metals accompanying PM10 may enter the circulatory system after being released into lung tissues. Metals may enter the cerebrospinal fluid through the circulatory system, overcoming the blood brain barrier and passing through the plexus choroid, and transfer to a specifc part of the brain (Karri *et al*., 2016). The risk level of heavy metals depends on the severity of exposure and biochemical metabolism in the brain (Shahsavani *et al*., 2012) The results of a study in mice showed that PM containing heavy metals such as lead, manganese, aluminum, and copper could enter the circulatory system, after respiratory exposure and then enter the target tissues such as blood, kidneys, and brain to subsequently cause damage (Li et al.,2012)

Many *in vitro* lung-on-a-chip models have been introduced in the past to study impacts of toxins under dynamic flow conditions almost all the previous models are PDMS based. PDMS absorbs hydrophobic biomolecules so PDMS based models fail to provide complete information of molecular markers and cytokine analysis in the culture medium, PDMS absorbs hydrophobic molecules in the media, absence of real time monitoring or probe based off line monitored sample analysis provide vague information of stress response. To study acute or chronic stress response of the cells, real time microscopy is required to analyze the morphological changes in normal cells which are lacked by previous microfluidic models.

Trans-epithelial electrical resistance (TEER) measurement is a rapid and conservative technique for the determination of integrity and differentiation of epithelial monolayers trans-well cultures because the electrical impedance across an epithelium is interrelated to the vigorous construction of tight junctions with neighboring cells. Cell monolayer integrity measurement by TEER has become a standard technique in trans-well culture system, technically TEER measurement of organ-on-chips is challenging because there is no valid and practical approach available. Micrometer sized closed microfluidic channels create hindrance in TEER measurements in organ-on-chips to contact epithelium. Therefore, measurement of permeability changes incessantly using TEER in microfluidic is almost impossible. Printed TEER electrodes integrated into PDMS based microfluidic devices have been developed but only a few have been used to monitor in situ within organ chips epithelial barrier function[9]. Conventional metal patterning techniques have been used in organ on chips microfluidic culture devices for construction of cell culture chambers around electrodes or integrating glass or polymeric substances. Previous studies with cells cultured in organ chips provide large variability in measurement, low sensitivity and they are affected by non-uniform cell cultures. TEER electrode location also significantly change in TEER values in these cultures, mathematical models can help to reduce these variations[10]. Therefore successful fabrication of a robust on-chip TEER sensing capability enabled us to measure barrier function electrochemically, this method measures electrical impedance it can also help to study other behaviors of the cells on a microfluidic chip such as cell proliferation, migration, ion channel activity, tissue conductivity and dissolved gases. PH sensors have been recently reported for real time monitoring by fabricating PDMS based organ chips with fully integrated electrodes. Embedded sensor in organ on chip platform are stringently required for future research applications for example many sensors such as

strain sensor, humidity sensor for health monitoring have been developed for implantable applications [11].

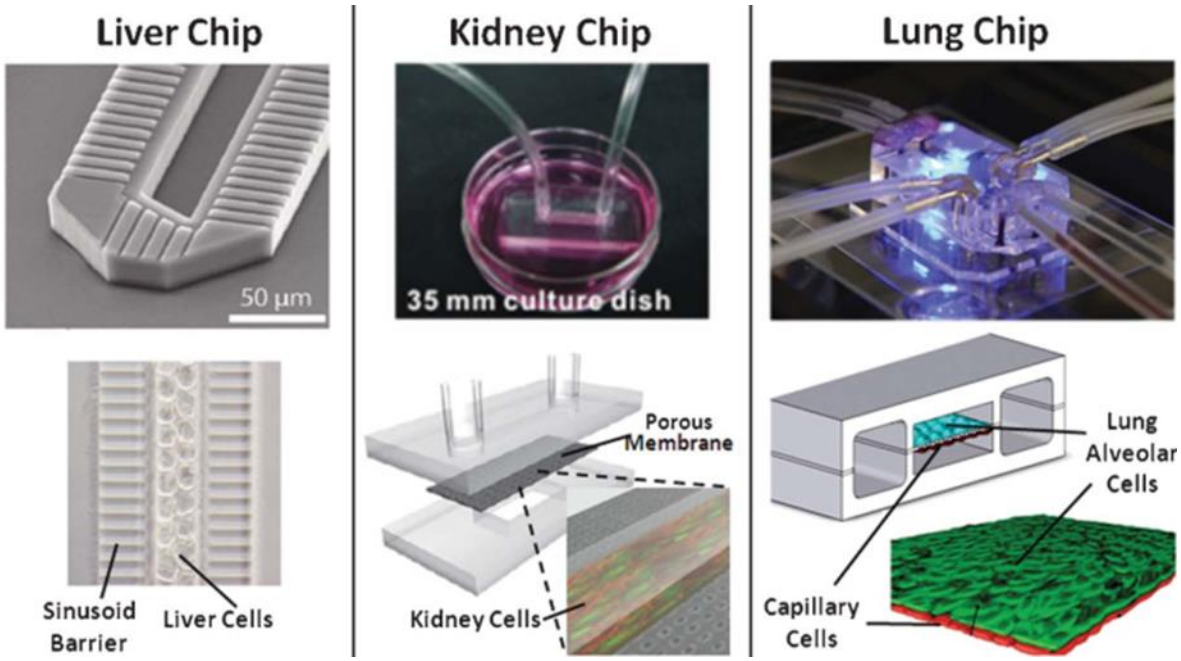

Figure 3Examples of Organ-on-a-chip devices for liver, kidney and lung. Source: design of Organ-on-a-chip devices for liver, kidney and lung. Source: Huh, D et al. Microengineered physiological biomimicry: organs-on-chips. Lab on a chip. 2012

PDMS absorbs hydrophobic biomolecules so PDMS based models fail to provide complete information of molecular markers and cytokine analysis in the culture medium, absence of online monitoring or probe based off line monitored sample analysis provide vague information of stress response. To study acute or chronic stress response of the cells online microscopy is required to analyze the morphological changes in normal cells which are lacked by previous microfluidic models. Trans-epithelial electrical resistance (TEER) measurement is a rapid and conservative technique for the determination of integrity and differentiation epithelial monolayers trans wells cultures because the electrical impedance

across an epithelium is interrelated to the vigorous construction of tight junctions with neighboring cells.

A multi-sensor lung cancer-on-chip platform for transepithelial electrical (TEER) impedance based cytotoxicity evaluation of drug candidates. The excellent transparency of ITO electrodes allowed for visual monitoring of cells on chip using a 3D-printed digital microscope, which has not been previously reported. An optical pH sensor was used for online monitoring of media pH. As a proof of concept, lung cancer NCI-H1437 cells were cultured on glass-based microfluidic chip and biosensors data were obtained in real-time[12]

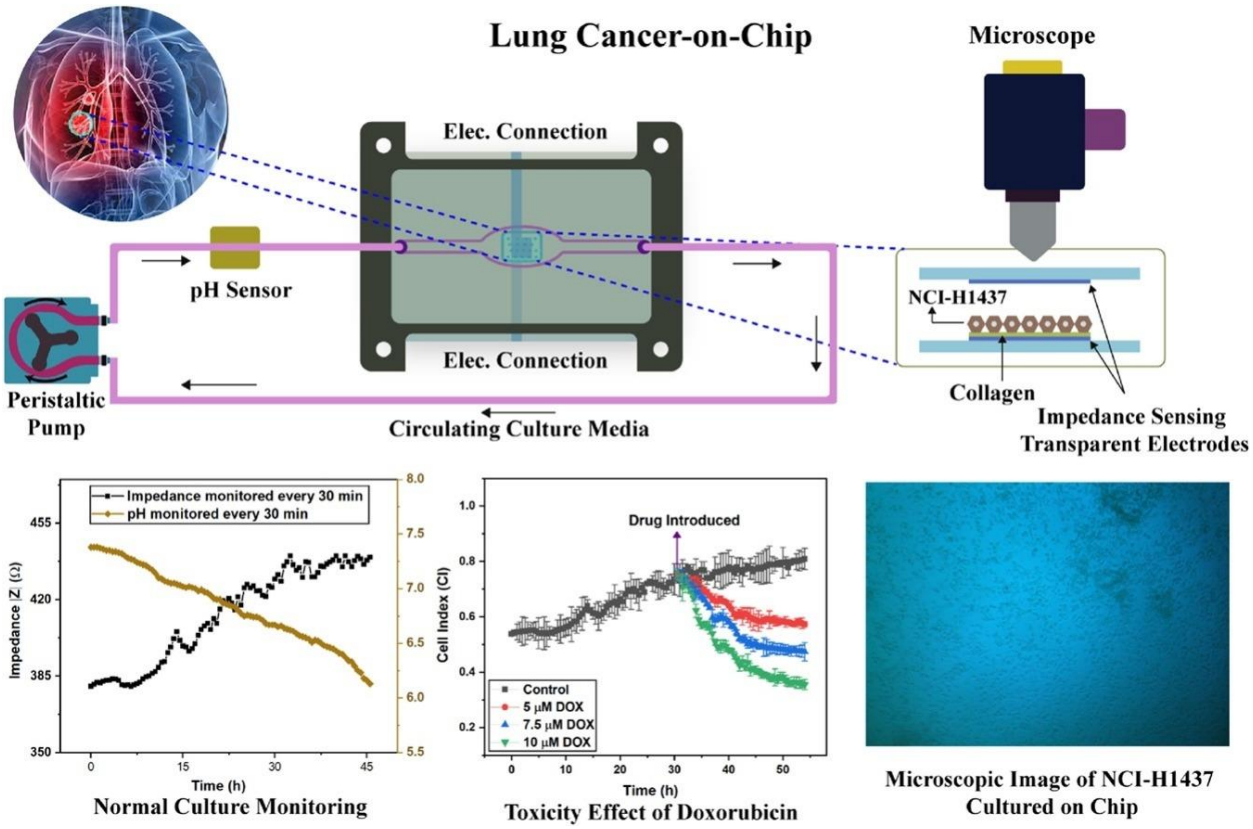

Figure 4 Lung cancer-on-chip with integrated biosensors for real-time microphysiological environment monitoring and cytotoxicity evaluation

2.1 Organ on chip technology

The organ-on-chip (OOC) is one of the 10 most emerging technologies and based on building physiologically biomimetic human organs in a microfluidic chip. Organ-on-a-chip technology has enormously appealed pharmaceutical industry, regulatory agencies and national defense agencies enormously with development of more than 28 organ-on-chip companies just in 7 years(Reardon, *et al* 2015). Drug screening in drug discovery process is the center of attention before clinical trials to predict the effects of drugs in humans. The cost of drug discovery is steadily increasing owing to the limited predictability of 2D cell culture and animal models. The convergence of microfabrication and tissue engineering gave rise to organ-on-a-chip technologies, which offer an alternative to conventional preclinical models for drug screening. Organ-on-a-chip devices can replicate key aspects of human physiology crucial for the understanding of drug effects, improving preclinical safety and efficacy testing. The development of the organ-on-a-chip technology brings together microfluidic engineering and basic human physiology to speed up drug screening as an alternative to animal testing. Microfluidic sensors facilitate real-time monitoring of the microtissue environment to extrapolate drug efficacy and toxicity.

2.2. Role of Microfluidics in Organ on chip technology

Microfluidics technology is a science that manipulates and processes microscale fluids precisely. It precisely control microfluidic (10−9 to 10−18 L) fluids in channels precisely that ranges from tens to hundreds of microns and recognized as a “lab-on-a-chip” [14]. The microchannel is small, and having large surface area and high mass transfer, including low regent usage, controllable volumes, fast mixing speeds, rapid responses, and precision control of physical and chemical properties makes it favorable to be use in microfluidic technology applications [15]. Microfluidics incorporate sample preparation, reactions, separation, detection, and basic operating units such as cell culture, sorting and cell lysis[16].

OOC is a biomimetic system that can mimic the environment of a physiological organ, with the ability to regulate key parameters including concentration gradients, shear force, cell patterning, tissue-boundaries, and tissue–organ interactions. The major goal of OOAC is to simulate the physiological environment of human organs[17].

It is becoming increasingly clear that the cell lines and animal models currently used for drug development and testing fall short in predicting the pathophysiology of human disease, personalized drug sensitivities of specific patient subgroups and off-target drug toxicity. For example, patient-derived tumour xenografts can undergo murine-specific tumour evolution when implanted in mice, questioning the validity of animal testing for cancer therapy[18]. Furthermore, the development of drugs for conditions affecting prenatal and newly born humans remains unaddressed owing to a lack of suitable models. It is also important to investigate teratogenic effects of drugs and environmental chemicals in the increasingly polluted world, which is currently not possible in humans. Therefore, new methods and approaches for drug discovery and health research are required.

One of the first papers detailing the use of organized cell cultures to study disease was published by Andre Kleber in 1991, reporting the construction of a ventricular myocardium through the patterned growth of cells in vitro, which enabled the first biophysical explanation of conduction block in the heart. The field of biomicrofluidics exploded in the late 1990s with the introduction of poly(dimethylsiloxane) (PDMS), which is an optically transparent, soft elastomer ideal for biological applications on the small scale. The concept of mimicking the organ-level function of human physiology or disease using cells inside a microfluidic chip was first published in 2004, when Michael Shuler and colleagues first demonstrated a cell culture analogue (CCA) system that captured the systemic interaction between lung and liver on a one square inch silicon chip[19].

This system in conjunction with a physiologically based pharmacokinetic (PBPK) model has the potential to supplement animal studies and serve as a human surrogate for the prediction of clinical outcomes. A range of microfluidic devices have since been developed, mimicking diverse biological functions by culturing cells from blood vessels, muscles, bones, airways, liver, brain, gut and kidney. In 2010, the term organ-on-a-chip was invented by Donald Ingber, who developed a microfluidic chip to capture organ-level functions of the human lung[19].

2.3 Current trends in OoC

This non-invasive approach enables the detection of small molecules and biomarkers within a complex biological environment with high sensitivity[20]. For example, a modular organ-on-a-chip device implementing such sensors can be used to automatically extract quantitative biochemical readouts from recirculating media with high specificity in a multi-

organ system. Electrodes can further be used to measure functional changes in tissues in real time. Instead of directly depositing sensory probes or electrodes using multiple lithography steps, a mechanical force sensor can be built by 3D printing of multiple materials in a single continuous step. Specifically, to probe the contraction of laminar cardiac tissues, a conductive ink composed of carbon black nanoparticles can be 3D printed and embedded in a soft thermal plastic polyurethane sheet that supports the growth of cardiomyocytes. The bending of the elastic sheet caused by cardiac cell contraction can lead to a change in the electrical resistance of the embedded conductive circuit[21]. Electrodes can also be used to study the barrier integrity of an endothelium. Gold-based or silver/silver-chloride-based [22] Electrodes can be incorporated in organ-on-a-chip devices to probe epithelial barrier integrity by measuring the *trans*-epithelial electrical resistance (TEER).

This quantitative readout is a useful metric not only for assessing the health of an endothelium but also for studying drug delivery and diffusion in tissues. The development of micro-sensors with high sensitivity presents an opportunity for organ-on-a-chip systems to effectively measure subtle, non-lethal changes in tissue functionality at the cellular level, which is an important advantage over animal testing

2.4 Physio-pathologically relevant human organ models

2.4.1 Lung on chip

Gas exchange in the lungs is regulated by the alveoli which can be challenging to reproduce in vitro. Microfluidics can establish extracorporeal lung models and lung

pathologies through accurate fluid flow, and sustained gaseous exchange. Current studies have focused on the regulation of airway mechanical pressure, the blood–blood barrier (BBB), and the effects of shear force on pathophysiological processes. Huh et al. produced a lung-on-a-chip model [23] using soft lithography to divide the chip into regions separated by 10 µm PDMS membranes with an extracellular matrix (ECM). The upper PDMS regions had alveolar epithelial cells, whilst the lower regions contained human pulmonary microvascular endothelial cells, thus mimicking the alveolar–capillary barrier. The structures of the membranes were altered under a vacuum to simulate expansion/contraction of the alveoli during respiration. Inflammatory stimuli were introduced into the system through neutrophils that were passed to the fluid channels.

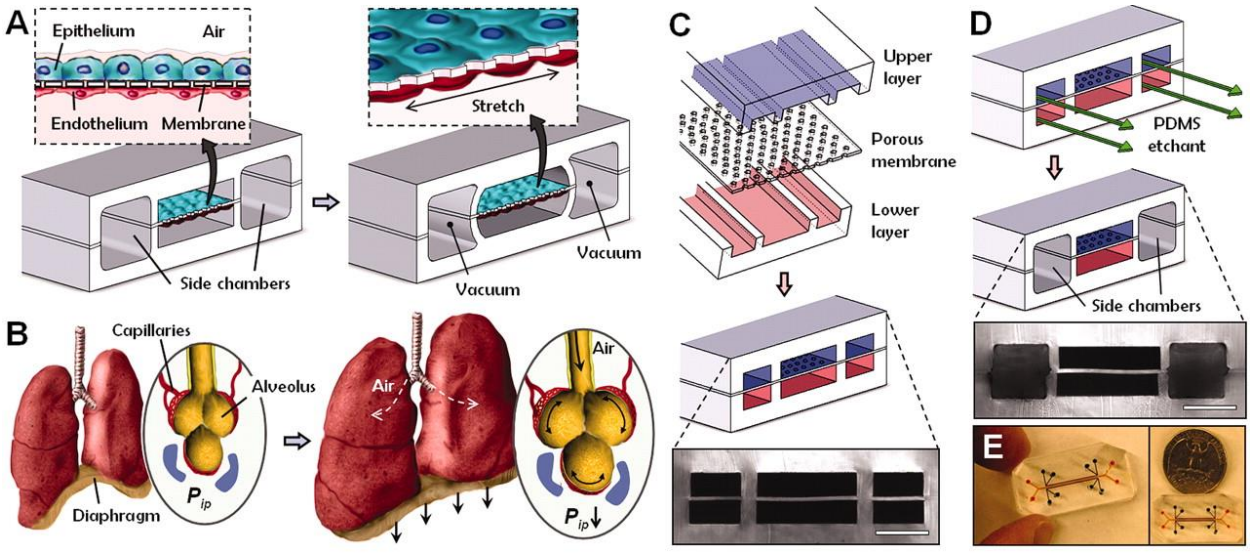

Figure 5.Biologically inspired design of a human breathing lung-on-a-chip. Reconstituting Organ-Level Lung Functions on a Chip, Science. Huh et al 2010.

This produced a pathological model of pulmonary edema through the introduction of interleukin-2 (IL-2). This highlights the utility of the OOAC models to improve current in vivo assays. In 2015, Stucki et al[24]reported a lung chip that mimicked the lung parenchyma.

The system included an alveolar barrier and 3D cyclic strain that mimicked respiration representing the first elastic membrane expansion model to simulate breathing.

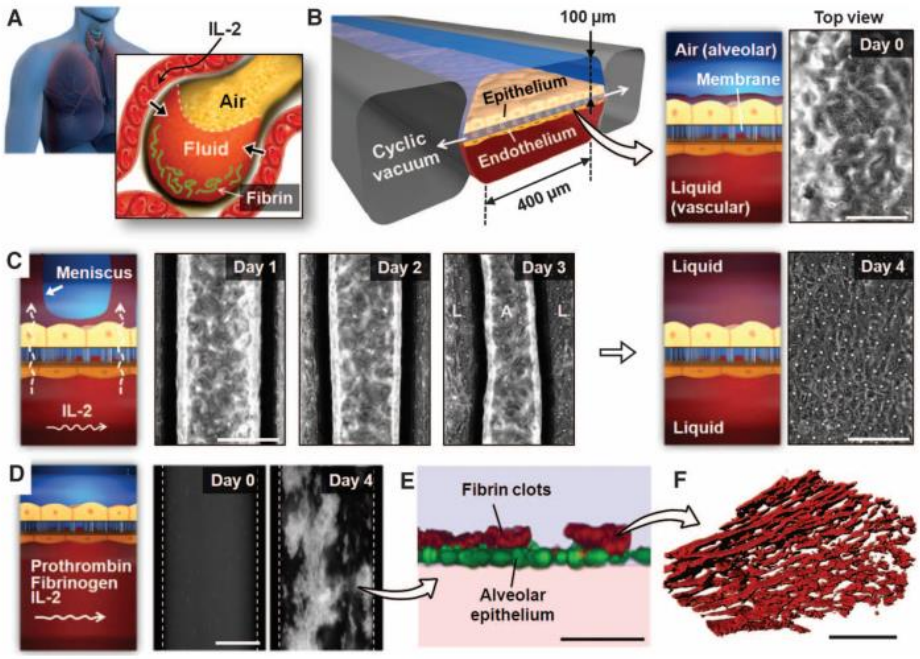

Figure 6 A microengineered model of human pulmonary edema

Blume *et al*. Produced 3D airway culture models that simulated pulmonary interstitial flow through the exchange of both fluid and media. This permitted more in-depth physiological studies of the epithelial barrier. This model utilizes a stent with a permeable filter as a single tissue culture chamber and combined multiple chambers for improved integration.

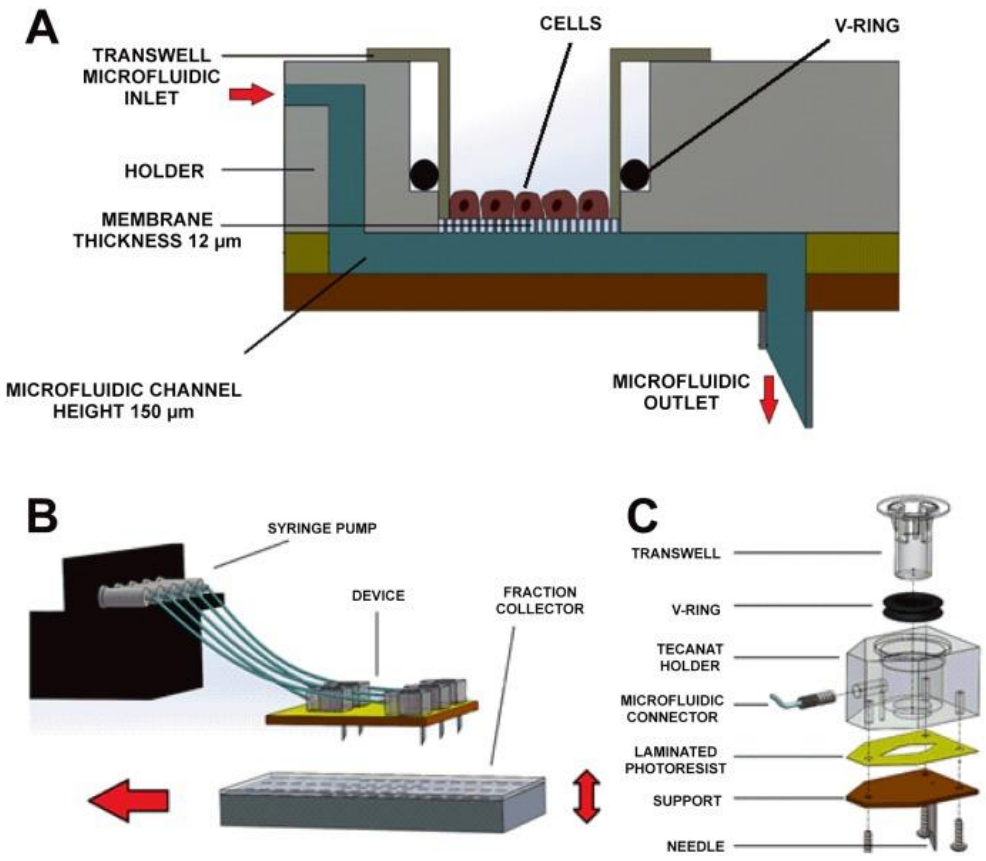

Figure 7 Design and assembly of the microfluidic culture system. Temporal Monitoring of Differentiated Human Airway Epithelial Cells Using Microfluidics Blume et al 2015 Plos one

In the lung-on-a-chip, whilst simulating lung gas–liquid interfaces and respiratory dilation through the microfluidic system, pressure can be applied to the alveoli and attached capillaries, providing a shear flow profile. This realistically simulates the lung environment. Humayun et al. cultured airway epithelial and smooth muscle cells at different sides of a hydrogel membrane to assess their suitability as a physiological model. The system was combined with microenvironment cues and toxin exposure as a physiological model of chronic lung disease. Yang et al. produced a poly(lactic-co-glycolic acid) (PLGA) electrospinning nanofiber membrane as a chip matrix for cell scaffolds. Given the ease of the system, it is applicable to lung tumor precision therapy and tissue engineering approaches was highlighted.

Lung tissue organ chips are useful as implantable respiratory assistance devices. Peng et al. designed lung assist devices (LAD) to permit additional gas exchange in the placenta for preterm infants during respiratory failure. The concept of large-diameter channels was achieved in the umbilical arteries and veins, providing LAD with high extra-corporeal blood flow. This has added utility because clinical trials for umbilical vasodilation thresholds were unethical. This study was the first to systematically quantify umbilical vessel damage as the result of expansion by catheters. Dabaghi *et al*. Performed microfabrication for microfluidic blood oxygenators using double-sided gas delivery to improve gas exchange. Oxygen uptake increased to 343% in comparison to single-sided devices. Xu et al. used a microfluidic chip platform to mimic the microenvironment of lung cancer with cancer cell lines and primary cancer cells and tested different chemotherapeutic drugs[17]. Recent study mimicked asthma in "small airway-on-a-chip" model models of human asthmatic and chronic obstructive pulmonary disease airways, therapeutics were tested and the chip model recapitulated in vivo responses to a similar therapy.

2.4.2 Liver-on-a-chip

Liver toxicity is another major cause of drug recalls, making up 32% of all cases of postapproval drug withdrawals between 1975 and 2007 (for example, trovafloxacin). The liver is the first organ that ingested drugs encounter after entering the bloodstream. Heterotypic (crosstalk between different cell types) and homotypic (crosstalk between the same cell type) interactions between hepatocytes and stromal cells are crucial for maintaining hepatocyte functions in vitro[25]. To investigate these cellular interactions, a micropatterning technique can be applied to deposit clusters of hepatocytes and stromal cells on a 2D surface. The balance of homotypic and heterotypic interactions can be fine-

tuned by varying cluster size and separation distance to keep hepatocytes functional in culture for weeks[25]. This technology was commercialized as HepatoPac by Hepregen, which was later acquired by Ascendance Biotechnology. In a collaborative study with Pfizer, HepatoPac tested 45 drugs using chronic drug exposure over 14 days to assess drug toxicity with a 65% success rate, which is a significant improvement over conventional platforms. However, the mechanisms of action of many drugs are modulated by inflammatory pathways. For example, a drug could indirectly affect liver cells by altering the secretion of histamine and cytokines from immune cells in the liver. Therefore, to improve the accuracy of toxicity screening, macrophage-like primary human Kupffer cells and hepatic stellate cells can be incorporated into the system to assess the effects of pro-inflammatory cytokines on liver toxicity. Intaglio-Void/Embed-Relief Topographic (InVERT) moulding enables the 3D micropatterning of tissue cultures and can be applied to pattern 3D aggregates of stromal cells and hepatocytes in a hydrogel. This hydrogel system shows good engraftment in mice and grows in size by 50-fold over 11 weeks, representing a substantial level of regeneration[25]. Organovo, a 3D bioprinting company, also builds 3D liver models for toxicity screening in collaboration with pharmaceutical companies (for example, GlaxoSmithKline, GSK). They apply 3D printing for cell patterning, which is especially useful for hepatocyte culture owing to the importance of heterotypic and homotypic cell interactions and the spherical morphology of these cell clusters. Moreover, the tissues printed by Organovo are large in size; they can generate a disc-shaped tissue with a minimal thickness of 250 µm which is ideal for the modelling of biochemically induced liver fibrosis and for assessment by histological sectioning, which is a standard technique used in the clinic to detect liver disease and drug toxicity. However, in a thick 3D tissue, chemical and oxygen gradients are formed, affecting cellular function and response. Rolled-up tumour tissue (tumour roll for

analysis of cellular environment and response, TRACER) that can rapidly assemble and delaminate can be used to spatially resolve, quantify and analyse the effects of hypoxic gradients on cancer cell metabolism and phenotype Hanging drop technology can be applied to create cell aggregates in suspension, which is a desirable microenvironment for liver, pancreas or tumour cells. This technology has been commercialized by inSphero and 3D biomatrix[19].

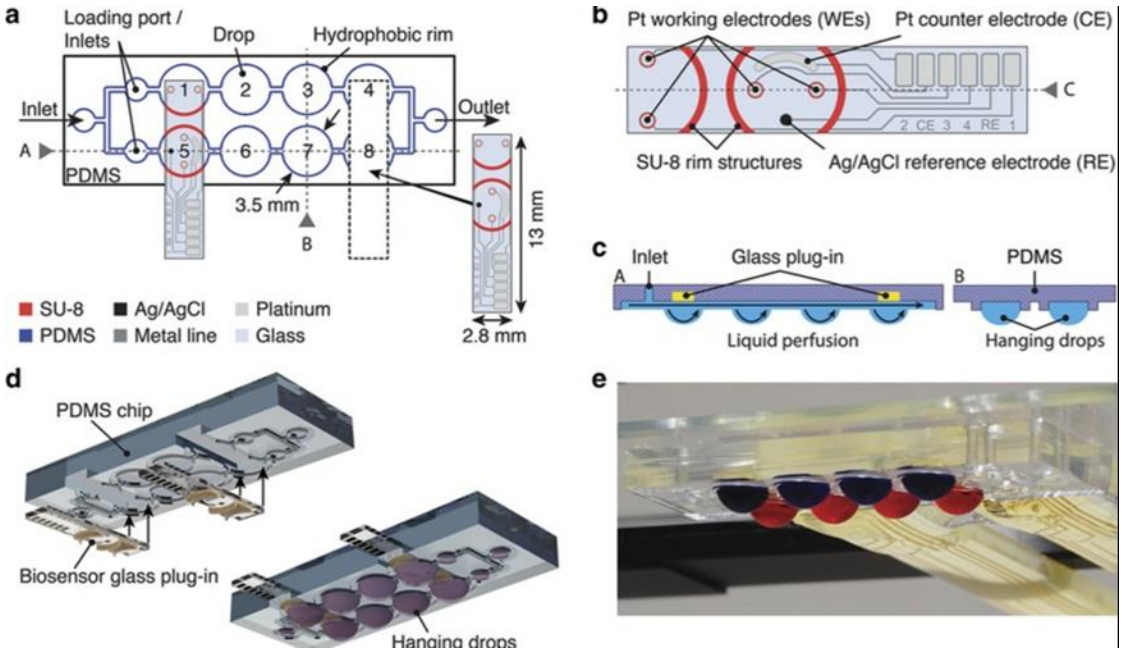

Figure 8Design and assembly of the microfluidic hanging-drop network and sensor glass plug-ins. (a) Schematic two-dimentional (2D) top view of the microfluidic 2×4-hanging-drop chip

Recently organ on chip pioneer company Emulate determine the cross species toxicity differences for a number of drugs in liver chip

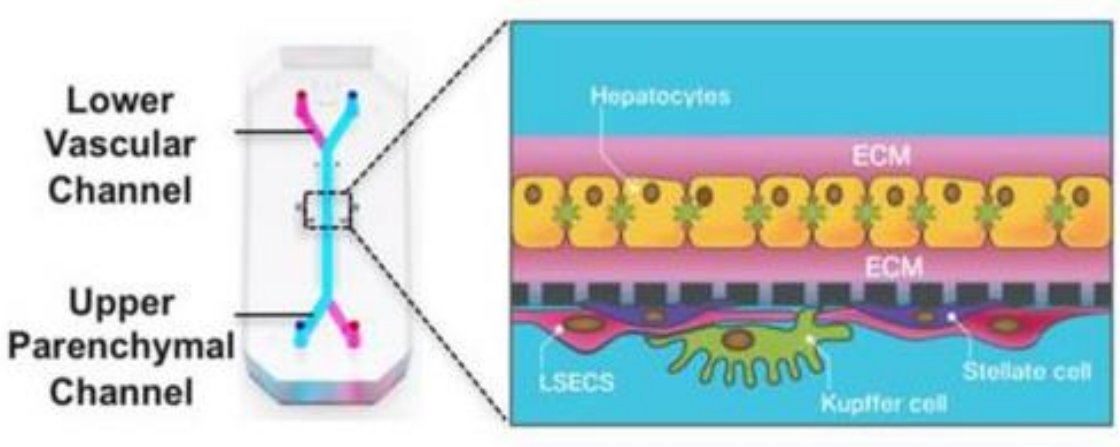

Figure 9 Schematic of the Liver-Chip that recapitulates complex liver cyotoarchitecture Primary hepatocytes in the upper parenchymal channel in ECM sandwich format and NPCs (LSECs, Kupffer, and stellate cells) on the opposite side of the same membrane in the lower vascular channel. Science Translational Medicine 06 Nov 2019

2.4.3 Kidney on chip

Kidney toxicity is one major cause of drug attrition and failure. Only 2% of drug development failures are screened in the preclinical stage and serious adverse effects in >20% of new medicines are discovered only after the clinical stages. The initial design of a published kidney-on-a-chip has two compartments. A top channel mimics the urinary lumen and has fluid flow, whereas the bottom chamber mimics interstitial space and is filled with media. Kidney cells are under much lower shear stress than the endothelial or lung cells. This device used rat distal tubular cells or MDCK cells, and its shear stress was ~1 dyn/cm2[26].

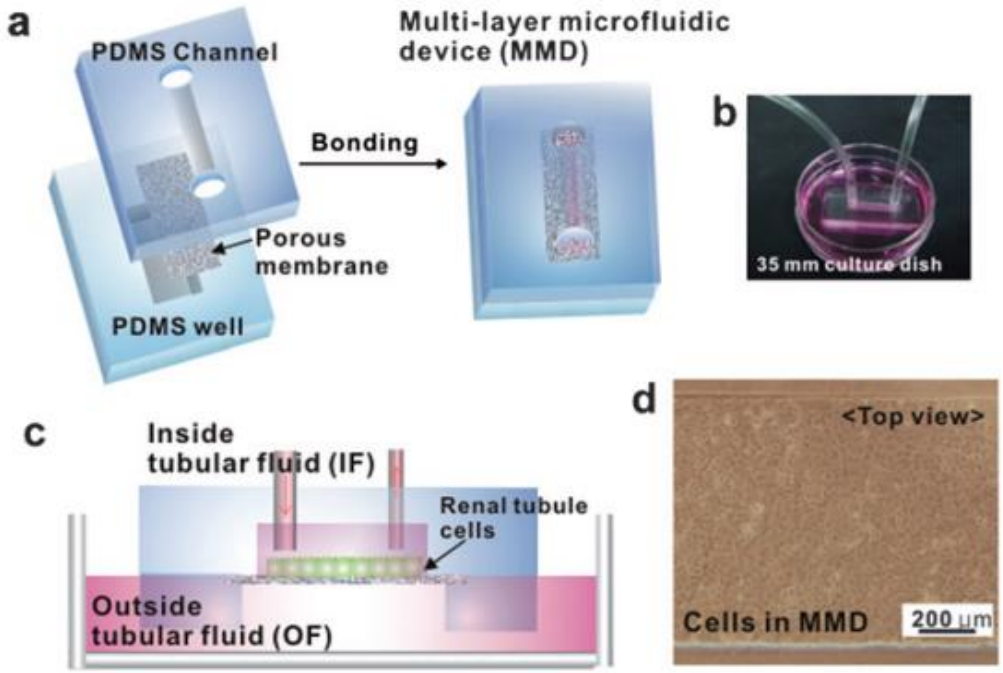

Figure 10 Fabrication and operation of a multi-layer microfluidic device

Kidney function impairment is accompanied by commonly predominant chronic diseases including hypertension and diabetes. High serum glucose induces cytotoxicity with the proximal tubule, which causes proximal tubulopathy (Gilbert 2017)Commonly prevailing chronic diseases mainly, diabetes, obesity, and hypertension put stress on the kidney's function (Bidani et al. 2013). Over time, the kidney's function is impaired under the influence of diabetes and hypertension (McCallum et al. 2019). In recent past, a few proximal tubule microfuidic models have been developed with the capacity to mimic both normal and diseased condition of the proximal tubule cells; however, PDMS was implemented for fabrication material in these chips (Jang et al. 2013; Sakolish et al. 2019; Vormann et al. 2018; Vriend et al. 2020)

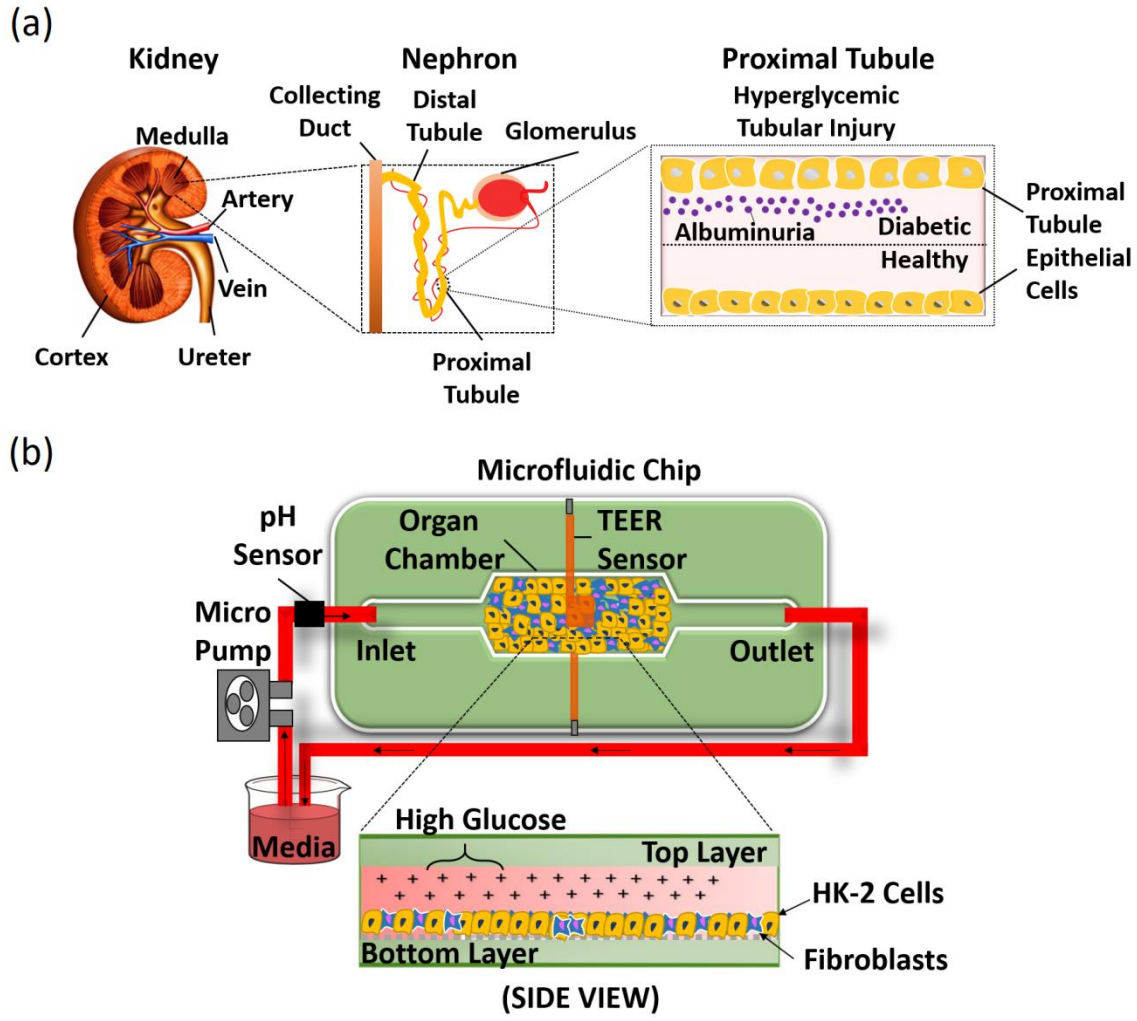

Figure 11 A Proximal tubulopathy. Cell injury caused by a Proximal tubulopathy. Cell injury caused by hyperglycemia leads to renal nephrotoxicity. b A schematic representation of the proximal tubule-on-a-chip model

2.5 Particulate matter based models

Exposure to small ambient particles like particulate matter (PM; aerodynamic diameter <10 µm) is of high concern in many industrialised countries. Many studies indicate that continuous exposure to air pollution and to PM significantly increases morbidity and mortality related to respiratory and cardiovascular diseases[4]. The relationship between daily

exposure to polluted air and augmented mortality became dramatically clear during the London fog episode in 1952 that was followed by a clear increase in mortality.

One possible explanation for the toxicity of atmospheric dust is that these particles can absorb pneumotoxic heavy metals as well as polycyclic aromatic hydrocarbons that can be found on their surfaces. Particle bound transport is considered to be a fundamental pathway for the distribution of these toxic compounds in the environment. Besides the larger particles with an aerodynamic diameter between 1 (PM_1) and 10 (PM_{10}) µm smaller particles of other size classes can also have detrimental effects on human health. During recent years the intensified use of nanotechnology led to the production of many new nanomaterials. The use of these materials may further increase exposure to ultrafine particles (aerodynamic diameter <100 nm) with potentially enforcing the risk for respiratory diseases. Nanomaterials and nanoparticles (NPs) (the first defined as a material with at least one dimension <100 nm and the latter as a material with all dimensions <100 nm) have become of primary interest for different kinds of industries. This downscaling enables the material to interact with the surrounding environment at a quantic level, opening the opportunity to generate material with new properties compared to the original bulk material. Despite a clear lack of knowledge on the toxicity of NPs, more than 1000 customer products already contain NPs (http://www.nanotechproject.org). NPs are supposed to have adverse effects on human health leading to an aggravation of pre-existing diseases, like asthma and some reports suggest that the toxicity of PM_{10} is actually mainly linked to the ultrafine fraction . Due to their small size, NPs can cross the alveolar barrier and affect the underlying cells or even enter the bloodstream thus causing damage in other parts of the body[27]

Among the mechanisms suggested to explain the adverse effects of particulates, the production of oxidative stress is likely of particular importance. Fine and ultrafine particles possess a high surface to mass ratio. In respect to this vast surface area per mass, the molecules that can be found on the surface can react more efficiently and in higher number with the surrounding environment, such as tissues, cellular membranes, etc. It is assumed that those surface molecules are in particular responsible for the observed oxidant capacity of particulates. Oxidative stress plays an important role in respiratory diseases, such as allergic asthma and rhinitis. The ability shown by some particles, such as diesel exhaust particles (DEP), carbon black or urban PM to produce reactive oxygen species

(ROS).

FINE DUST (PM10-LIKE)ERM-CZ 100		
PAH	Mass Fraction	
	Certified value [mg/kg]	Uncertainty [mg/kg]
Benzo[a]anthracene	0.91	0.07
Benzo[a]pyrene	0.72	0.05
Benzo[b]fluoranthene	1.42	0.14
Benzo[j]fluoranthene	0.75	0.14
Benzo[k]fluoranthene	0.67	0.06
Dibenzo[a,h]anthracene	0.18	0.04
Indeno[1,2,3-c,d]pyrene	1.07	0.10
benzo[b]fluoranthene		
benzo[k]fluoranthene		
benzo[j]fluoranthene3)	2.84	0.21

Figure 12Chemical composition of PM10 (ERM-CZ100)

FINE DUST (PM10-LIKE)		
PAH	Mass Fraction	
	Certified value [mg/kg]	Uncertainty [mg/kg]
Arsenic	7.1	0.7
Cadmium	0.90	0.22
Lead	113	17
	58	7

Figure 13 Chemical composition of PM10 (ERM-CZ120)

Exposure to fine and ultra-fine ambient particles is still a problem of concern in many industrialised parts of the world and the intensified use of nanotechnology may further increase exposure to small particles. Complex *in vitro* coculture systems may be valuable tools to study particle-induced processes and to extrapolate effects of particles on the lung. A system consisting of four different human cell lines which mimics the cell response of the alveolar surface *in vitro* was developed to study native aerosol exposure (Vitrocell™ chamber). The system is composed of an alveolar type-II cell line (A549), differentiated macrophage-like cells (THP-1), mast cells (HMC-1) and endothelial cells (EA.hy 926), seeded in a 3D-orientation on a microporous membr*a*ne[28].

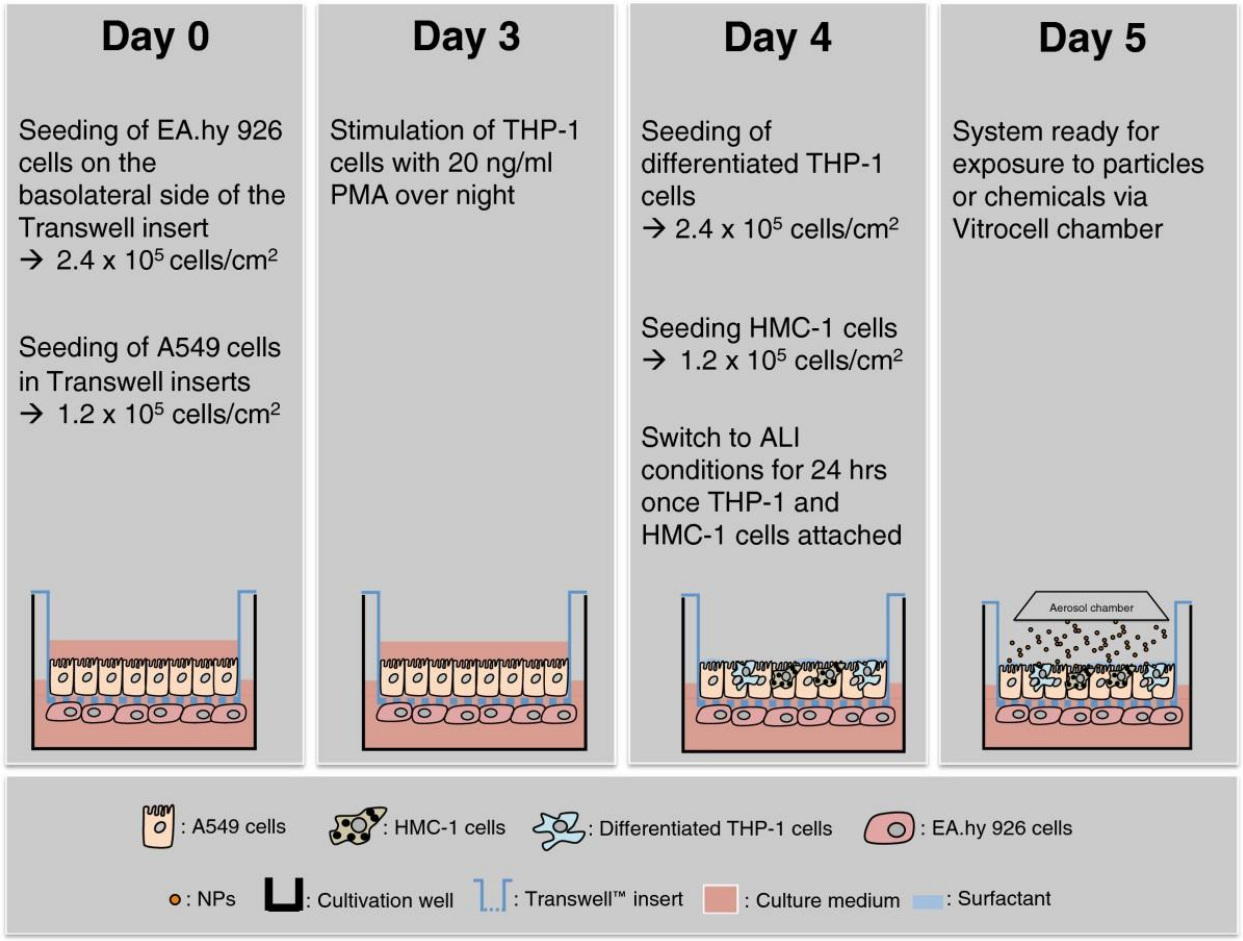

Figure 14 3D tetraculture system mimicking the cellular organisation at the alveolar barrier to study the potential toxic effects of particles on the lung

A PM2.5 exposure model to evaluate the pulmonary risk of fine particulate matter exposure in an organotypic manner with the help of 3D human lung-on-a-chip. By compartmentalized coculturing of human endothelial cells, epithelial cells, and extra cellular matrix, our lung-on-a-chip recapitulated the structural features of the alveolar–blood barrier, which is pivotal for exogenous hazard toxicity evaluation. PM2.5 was applied to the channel lined with lung epithelial cells to model the pulmonary exposure of fine particulate matter. The results indicated acute high dose PM2.5 exposure would lead to various malfunctions of the alveolar-capillary barrier, including adheren junction disruption,

increased ROS generation, apoptosis, inflammatory biofactor expression in epithelial cells and endothelial cells, elevated permeability, and monocyte attachments.[29]

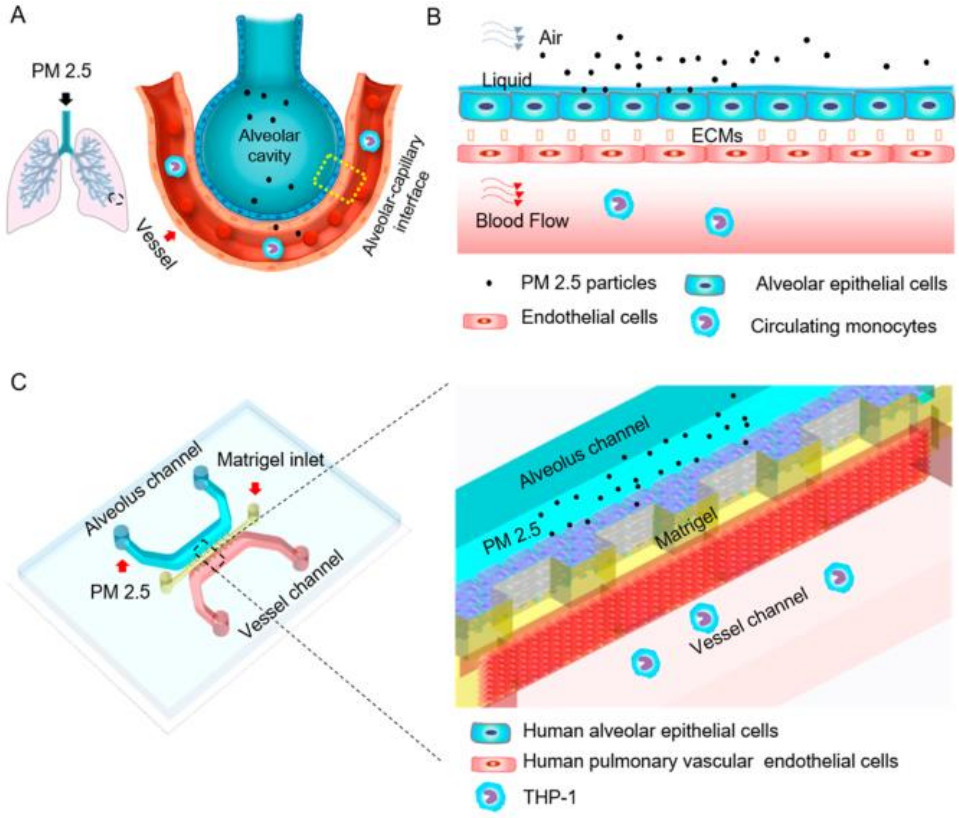

Figure 15 Schematic illustration of the PM2.5 exposure model on the lung-on-a-chip. (A) Pulmonary PM2.5 exposure in vivo. (B) Diagram of PM2.5 particles depositing in the alveolar-capillary barrier in vivo. (C) The design and structure of the lung-on-a-chip for PM2.5 exposure.

3. Materials & Methods

3.1 Materials:

Particulate matter particles PM10 reference material organic components ERM CZ-100 and inorganic ERM CZ-120 were purchased from European Joint research commission JRC were characterized for their size with scanning electron microscopy (MIRA-3

TESCAN).Three concentrations of both materials were prepared according to guidelines provided by daily update of climate control department South Korea, According to these guidelines mild, average and poor conditions are available Following these concentrations particulate matter doses for exposure were determined for analysis. Stock solutions of particulate matter material were prepared in Class II biological safety cabinet to ensure the endotoxin free and sterile environment, 151*µg/ml* of particulate matter material was suspended in alveolar epithelial complete growth medium and was sonicated in probe sonicator for 60 minutes for disagglomeration, Further diluted for two less concentrated particulate matter solutions by adding more media with resulting concentrations of 37.5*µg/ml* and 7.5*µg/ml* respectively. Particulate matter was kept at 4°C either diluted or in original form.

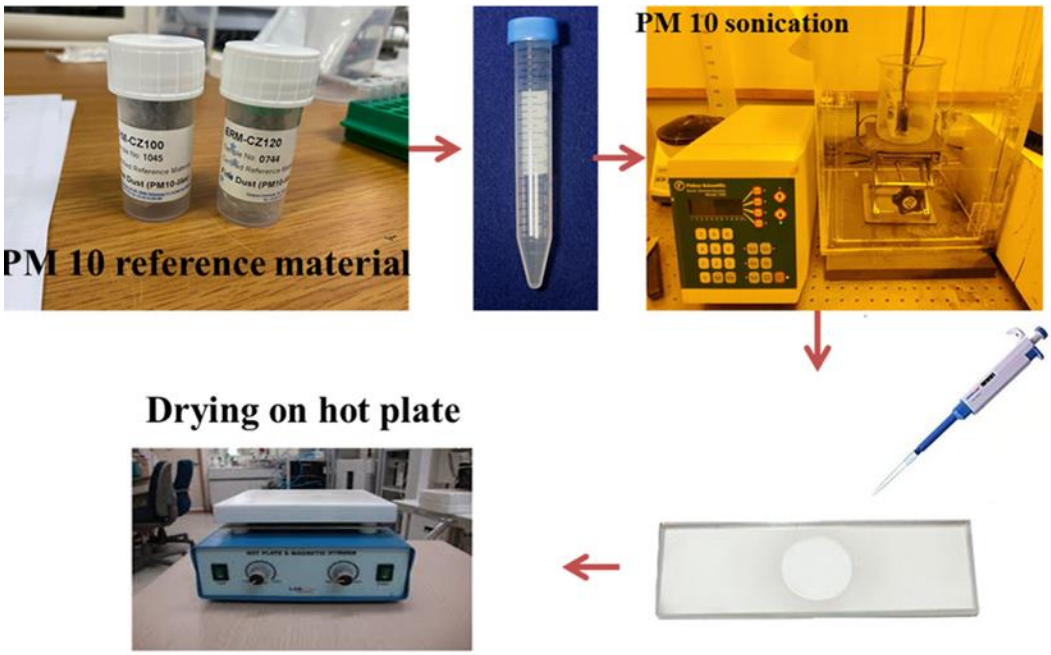

Figure 16 PM10 reconstitution and SEM Sample preparation procedure

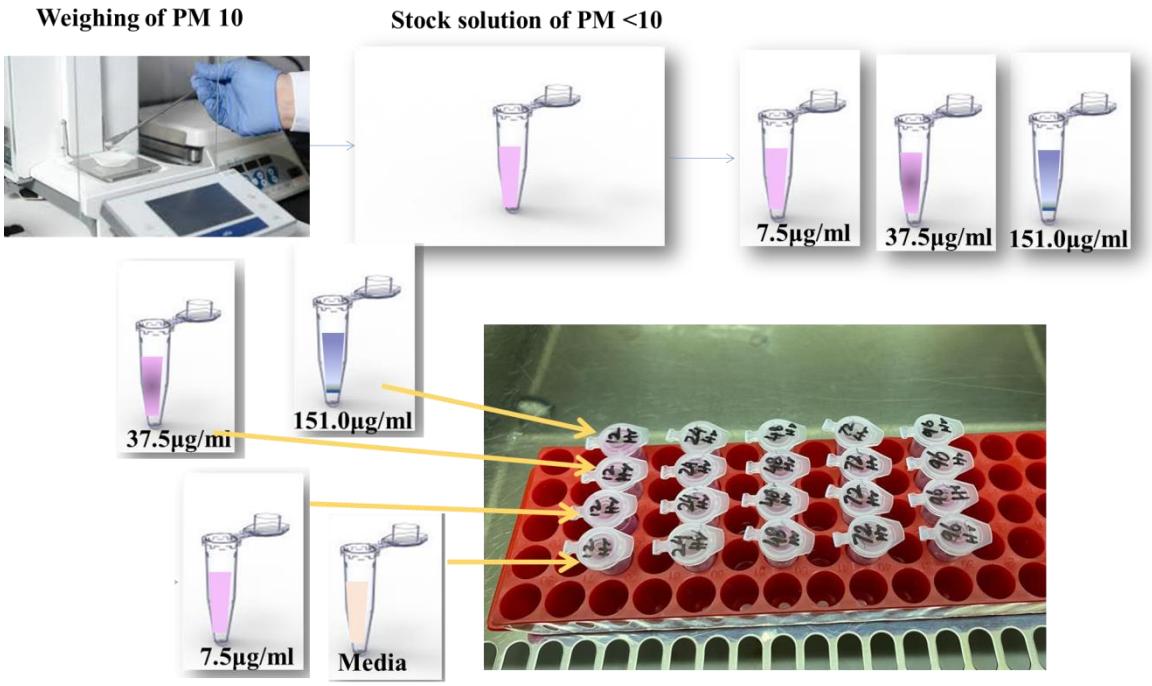

Figure 17 Preparation of PM 10 stock solution and concentrations

3.2 Methods

3.2.1 Microfluidic chip fabrication

Chip is made up of combination of two soda lime glasses 1.1mm thick, 41 mm wide and 56mm long. Channel for cell culturing was printed on the bottom glass of the chip

15mm channel area was allocated for cell culture compartment. To launch a TEER sensor, indium tin oxide (ITO) coating was printed to make a square electrode of 4 mm length with a thickness of 500 nm. Screen printing technique was used for printing ITO 112 on the glass. 3D inkjet printer was used to print the pattern of silicon elastomer (Musil 113 medical grade silicon MED-6033) (900 nm width) to create channel and cell culture chamber on the chip. Top and bottom chip glasses were fixed in a chip holder at a place where ITO electrodes are exactly crossing each other to complete circuit for measuring electrical resistance. One ITO based TEER electrode is $4mm^{2.}$

3.3 Microscope development & Sensor development

The impedance was measured in Ohms (Ωmm2). LabVIEW based software was used to monitor the TEER data from the chip and the connectors were coupled to the ITO electrodes. A120 portable microscope was developed for real time monitoring of cell growth on transparent ITO based TEER sensor printed chip, A commercially available Plan Achromatic Objective 121 (AmScope TM) with 10X magnification power, a white LED for light source, and a SCMOS series 122 USB2.0 eyepiece camera (ToupTek TM) were assembled in a 3D printed assembly as shown in Fig. 123 3. A blue wavelength 469±17.5nm filter was used. A camera control software was used for high speed visualization of the images and video processing ToupView (ToupTek TM).

pH sensor was developed for real-time pH monitoring of media. A white LED was inserted in a 3D printed assembly with a photodiode and an optical filter. The pH measurement was calculated on the principle of change in light intensity. A media carrying biocompatible microfluidic, extremely transparent, tube was passed through the sensor. Sensor was programmed to measure the minor discrepancies in color of media with changes

in phenol red color due to the acidification of media with time. An Arduino microcontroller was used to quantify an optical signal. To calibrate and characterize the optical pH sensor standard pH media samples ranging from 6.0 to 8.0 were used. A peristaltic pump was connected to the chip for constant media circulation to mimic dynamic conditions. The shear stress on the cell monolayer induced by media was calibrated to mimic the alveolar environment. The fluid shear stress in in-vivo human lung physiology has been characterized as 8 Dyne/cm2. The media flow rate was regulated at 80µl/min to maintain the 8 Dyne/cm2 shear stress upon the monolayer of lung epithelial cells. The media shear stress induced in the microchannel of the designed chip was calculated by the use of following equation;

$$\tau = 6\mu Q/(wh^2)$$

In this equation, µ represents the viscosity of the media, Q represents the media flow rate, w represents the width and h represents the height of the microfluidic channel.

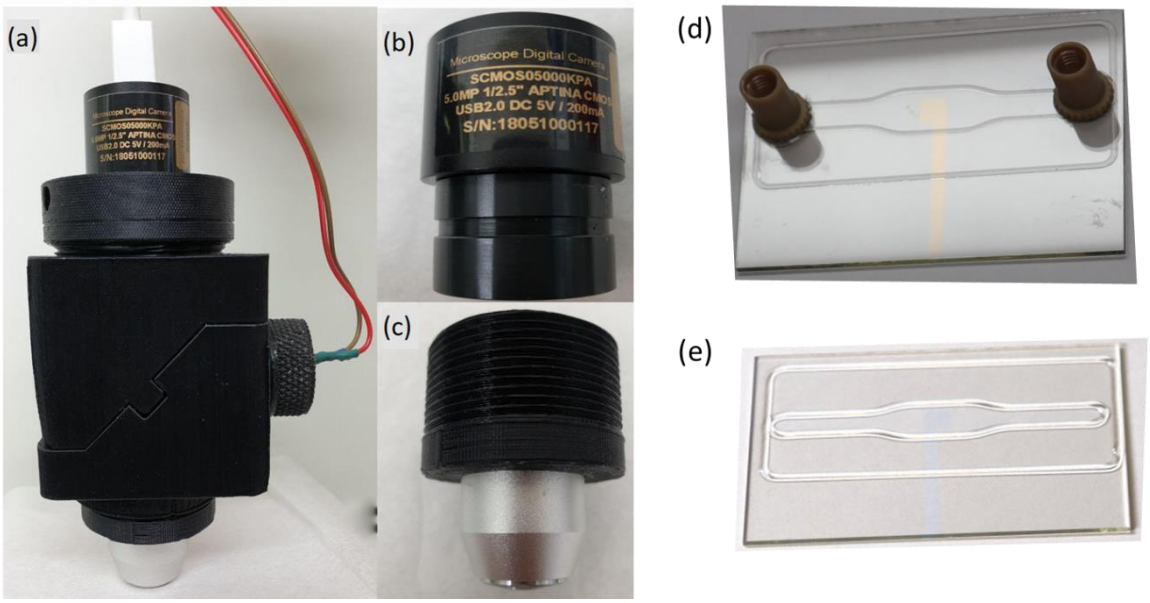

Figure 18 Extended view of Real time microscope and chip components

Optical pH sensor was attached to measure real-time pH before the media inlet. Connectors were immobilized upon glass chip with epoxy raisin through which tubing was connected to chip for the media circulation controlled by peristaltic pump.

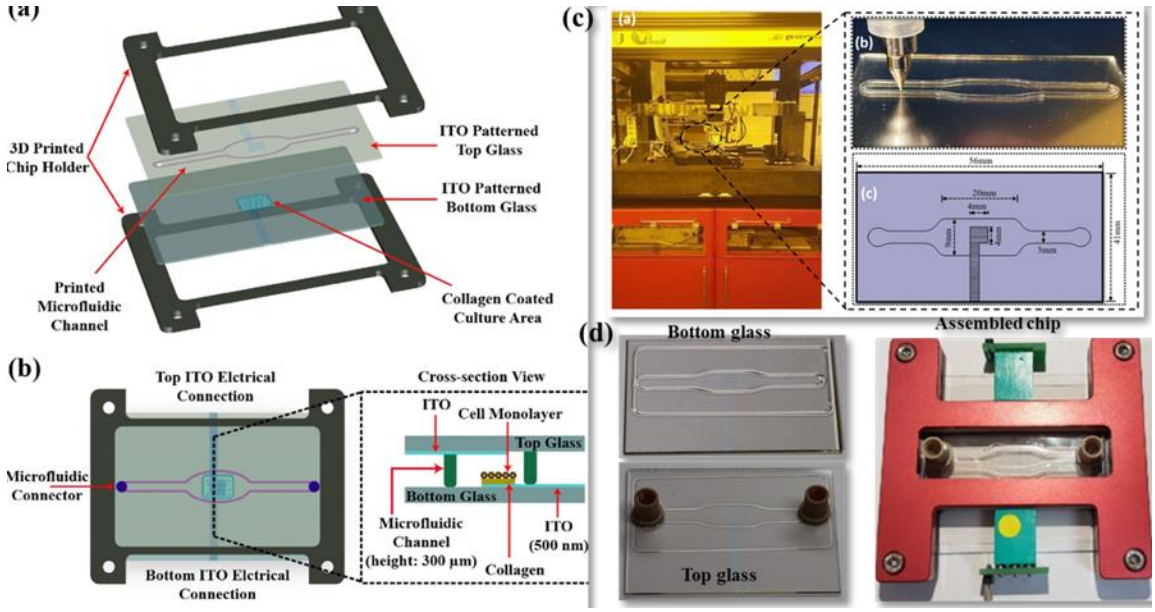

Figure 19Microfluidic glass chip fabrication. (a) Expanded schematic view (b) Schematic assembly - top view and cross section view (c) 3D channel printing system

3.4 Microfluidic cell culture

3.4.1 Microfluidic cell culture maintenance of lung on chip

HPAEpiC's(Cat#3200) were purchased from science cell and revived according to manufacturer's protocol, Poly-L lysine (Sigma Aldrich) was coated on T-25 flask(Corning) at concentration of 2µg/cm^3 incubated at 37°C overnight and flask was rinsed before adding culture medium containing Alveolar epithelial cells medium (AEpiCM, Cat. # 3201) minimal eagle medium, Epithelial growth supplement (5ml), 10% FBS,1%pencilin streptomycin

solution, with 5% carbon dioxide at 37°C. Before seeding cells on chip bottom glass was sterilized for 1 hour in UV and ECM Collagen solution type-I from Rat tail (Sigma Cat # C3867) was coated at concentration of 10µg by using 0.01% solution in DPBS overnight.

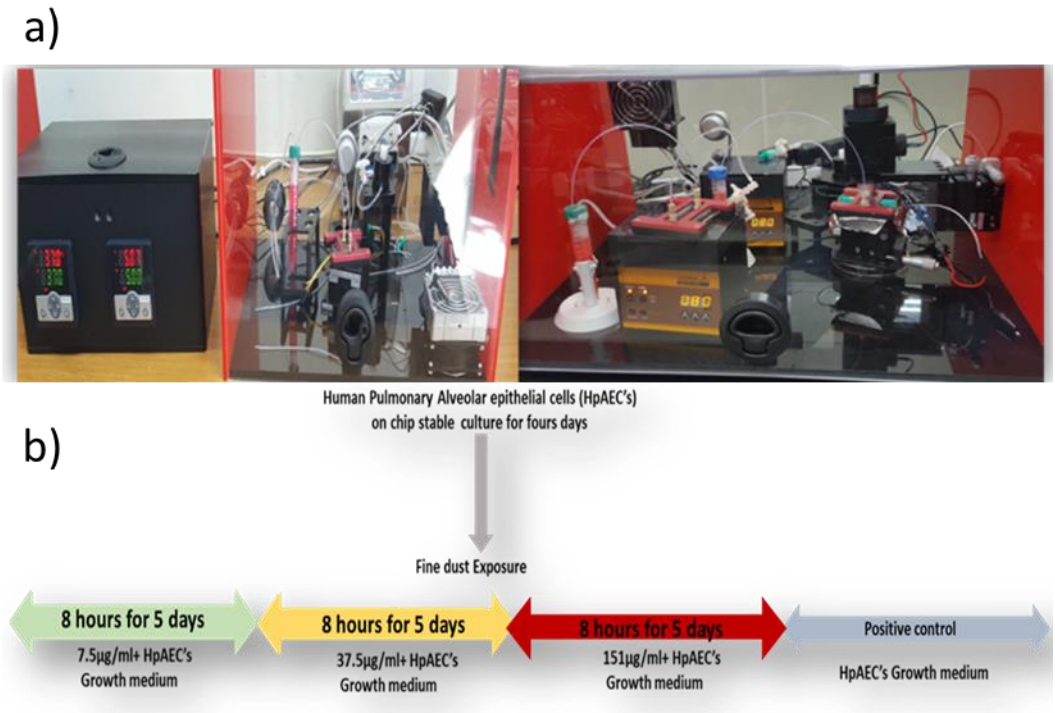

Figure 20 a. Organ on chip platform attached with Peristaltic pump, and portable microscope, with controlled temperature and carbon dioxide. b. Fine dust exposure scheme. Green arrow is representing good condition, whereas yellow is bad and red is worst respectively.

3.5 Human organs on chip models development

3.5.1 Lung on a chip

At reaching confluency <90 % at passage 2 HPAEpiC's+ small airway epithelial cells at density of $3.27x10^5$ were seeded on to the chip initially cells were allowed to adhere to the ECM coated channel of the chip for 4 hours, whereas for mimicking lung cancer on chip HPAEpiC's+ small airway epithelial cultured and allowed to adhere for 4 hours, and then A549 cancer cell were seeded on the chip then chips was introduced to the microfluidic platform for continuous circulation of media with help of peristaltic pump at 120µl/hour, TEER, pH sensors and microscope for online monitoring were attached to the chip after assembling the chip components after 12 hours media flow was increased to 80µl/min, after 48 hours fresh media was added to media reservoir. All the experiments were performed in triplicates.

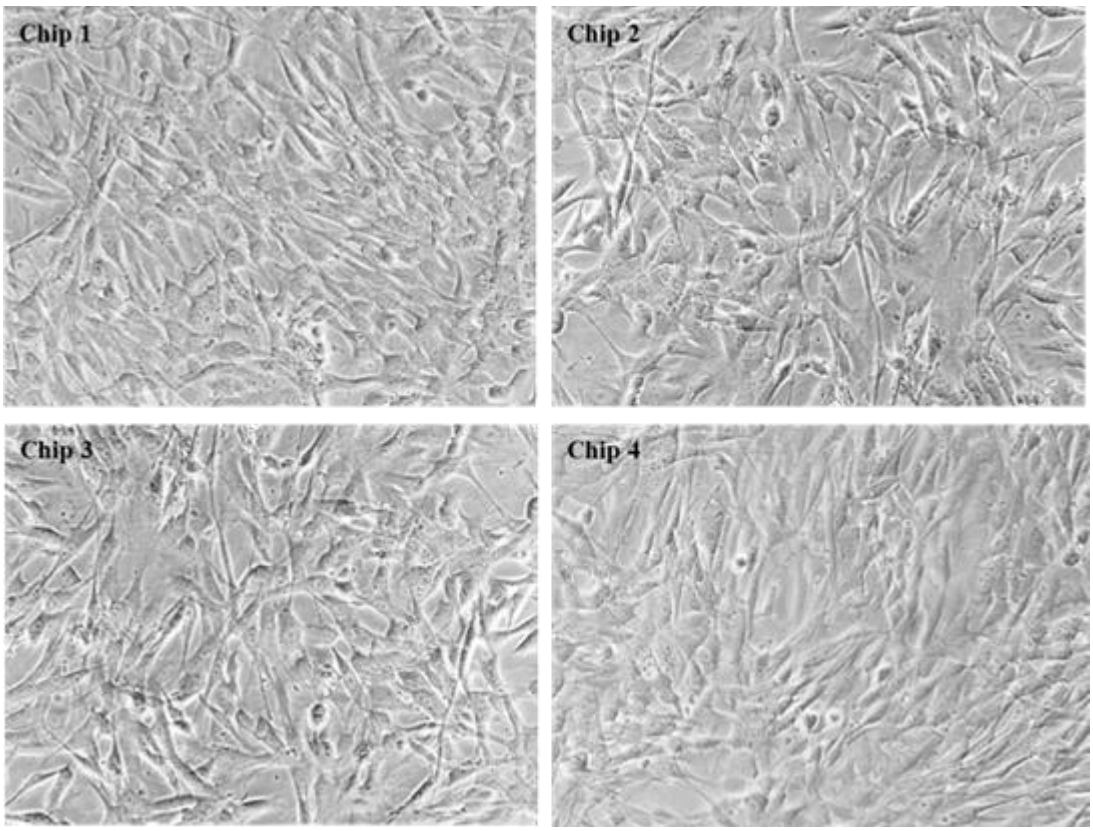

Figure 21 HPAEiC's and small airway epithelial cells on chip after 4 hours of attachment on the chip

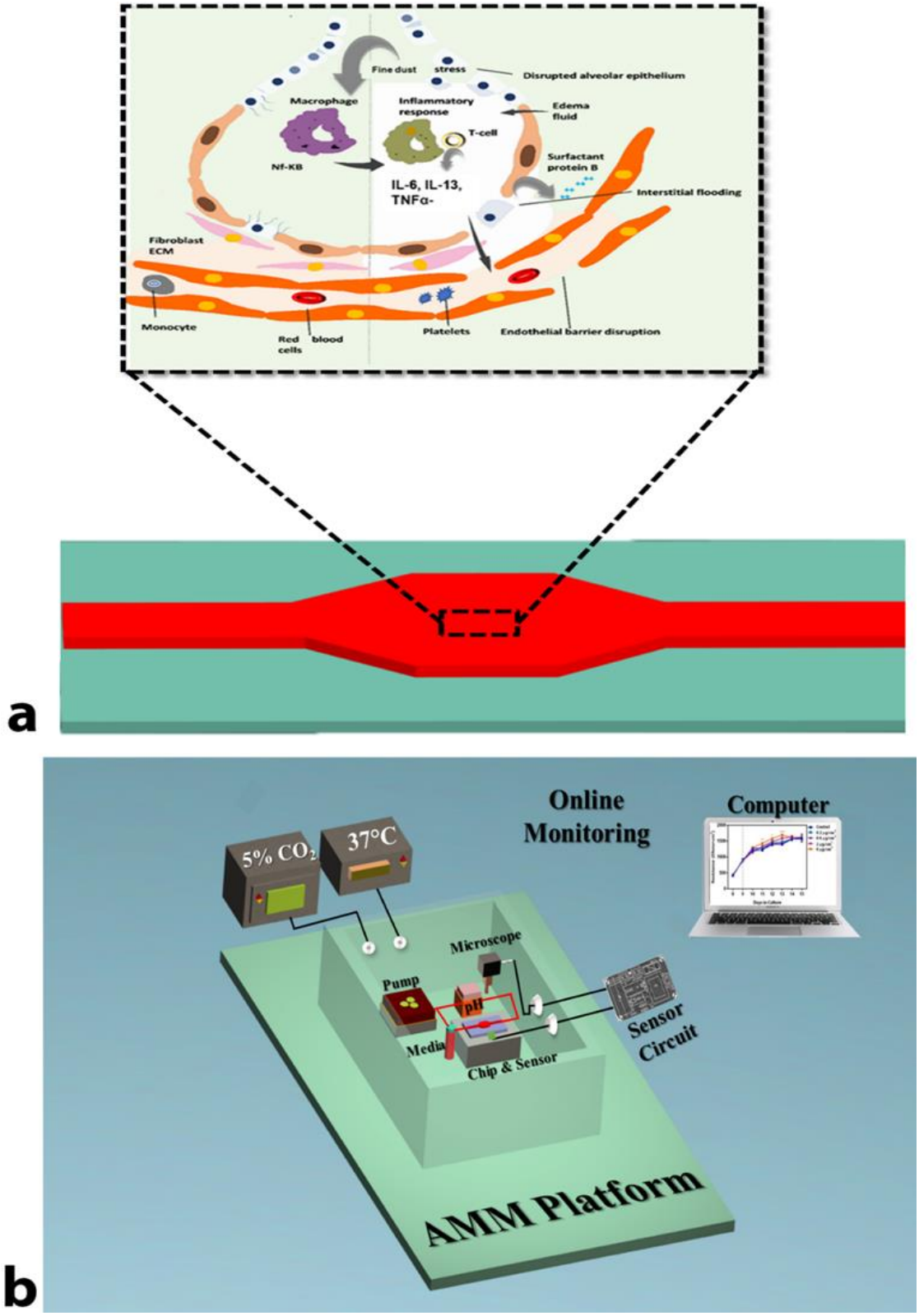

Figure 22. a. *Schematic Illustration of lung on microfluidic chip mimicking Particulate matter effects on human lung. b) Experimental set up of lung on chip microfluidic device.*

3.5.2 Pathological models development

3.5.3 Exposure scheme of fine dust

After 4 days of stable culture of HPAEpiC's on chip evaluated by impedance values of the TEER sensor, pH sensor and online microscope 3 chips representing moderate (7.5µg/ml), poor (37.5µg/ml) and very poor (151µg/ml) conditions of fine dust were allowed to exposed to fine dust containing culture medium, for consecutive 8 hours daily for 5 days, to mimic daily exposure of fine dust to human lung, was then exchanged with normal medium after exposure. All the chips were kept in same culturing conditions except different concentrations of fine dust excluding control chip.

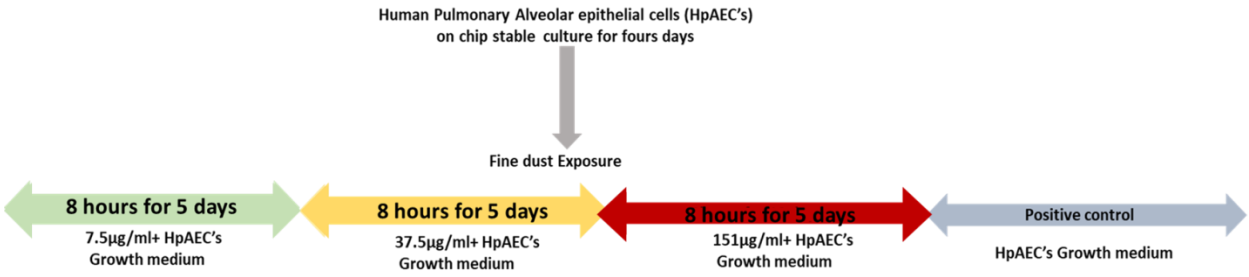

Figure 23 Particulate matter exposure schemes

3.6 Toxicity analysis

3.6. 1 Determination of Membrane barrier integrity:

Epithelial cell tight junctions' integrity was characterized by impedance values provided by in-house developed TEER sensor for online monitoring. Lung epithelial cells

were stained for immunofluorescence analysis by staining for tight junction's epithelial cell marker occludin conjugated Alexa flour 594 (Sigma (OC-3F10) For immunostaining cell were washed with PBS for 5 times and fixed with 4% paraformaldehyde for 15 minutes permeabilized with 0.2% triton X-100(Sigma) for 20 minutes and block with 5% BSA in PBS for 1 hour at room temperature and incubated for 4 hours with Occludin conjugated alexaflour 594(1:200) after incubation viewed under confocal laser scanning microscope

3.6.2 Immunofluorescence Analysis of compromised barrier integrity

Lung epithelial goblet mucus producing and ciliated cells were stained for immunocytochemical analysis cells were washed with PBS and fixed with 4% paraformaldehyde for 15 minutes washed with PBST for 3 time and permabilized with 0.1% triton 100 -X for 20 minutes at room temperature and block with 1 % BSA for 30 min at room temperature followed by MUC5AC Monoclonal Antibody (45M1)1:1000 and Anti-β tubulin IV (ab11315) abcam (1:500) antibodies and secondary Alexa flour Goat anti mouse (H+L) 488 Green and Goat anti-rabbit 594(H+L) red respectively for proper morphological analysis and images were taken under laser scanning confocal microscope(Zies Gremany) .

3.6.3 Analysis of cytokines release and ROS representing diseased conditions

Our particulate matter model on chip mimicking in-vivo diseased conditions was characterized by complete information of cytokine signaling. Neutrophil uptake increases on the onset of inflammation in airway cells so here is the list of cytokines produced as consequence of allergy and asthma TNF-α, IL-6, IL-13, Mucin and Reactive oxygen species(ROS) detection is the indicator of incidence of asthma due to prolonged exposure of

particulate matter to airway cells, presence of IL-13 provide data about the incidence of COPD, TNF alpha , for oxidative stress and ROS production leading to apoptosis which ultimately results in invasion of cancer in the tissues. Mucus metaplasia and mucus hypersecretion in human lung airway are pathological changes which occurs on the onset of a severe respiratory disease asthma. These are associated with the $CD4^+$ Th2 type of immune response activation in the lung. This immune response is evaluated by IL-13 secretion, with minimal production of the Th1 type of cytokines (e.g. IFNγ). The destiny of effector $CD4^+$ T cells is decided by the cytokine environment, which is one of the most important factors, so that the local immune response is affected by cytokines production by lung physical foundations. Although, lung epithelial cells are not part of the immune system but also contribute to the type of immune response by secreting explicit cytokines. One of the cytokines that is produced by lung epithelial cells is IL-6. IL -6 is the cytokine that is produced by lung epithelial cells and asthmatic patient's data provide relatively increased secretion of IL-6 as compared to healthy controls. In response to PM exposure IL-6 and tumor-necrosis-factor alpha (TNF-α) key intermediaries of the inflammatory response of lung epithelial cells in many in-vivo, in-vitro and human sample based studies which may leads to the increased tumor growth and invasion of cancer cells to other tissues.

In current study TNF-α, IL-13, IL-6 and Mucin were selected as biomarkers for asthma and COPD all the cytokines were detected in media samples collected after every 24 hours from all control and experimental media reservoirs, TNF-α, IL-13, IL-6 ELISA was performed by ELISA kits by standard protocol of manufacturer and ELISA for mucin was performed by sandwich method, Cytokine analysis was also performed for lung cancer chips by using same methodology as healthy lung chips (33).

3.7 DCFDA assay for ROS analysis

As a consequence of cell damage and functional impairment activated defense mechanism release production of intracellular Reactive Oxygen Species (ROS) and anti-oxidant species, pro- and anti-inflammatory cytokines, and induce genotoxicity. ROS are responsible for mitochondrial damage and for making cellular environment more acidic environment which leads to the incidence of chronic inflammation and cancer long term exposure to the xenobiotic and air pollutants are responsible of many respiratory diseases such as COPD, Asthma and cancer. For ROS evaluation on exposure to fine dust we have analysed three concentrations of fine dust after four days of exposure along with normal healthy control and All the chips were washed with PBS and the cells were incubated at 37 °C, in 5 % CO2 with 50 µM of a 5-(and-6)-chloromethyl-2′, 7′-dichlorodihydrofluorescein diacetate (CM-H2DCFDA) (Sigma D6883) probe in PBS and incubated for half an hour. After incubation the chips were washed with PBS and incubated for 5 min in 90 % Dimethyl Sulfoxide (DMSO) (Sigma-Aldrich, D2438) in PBS.Cell were washed and then visualized under laser scanning confocal microscope.

4. Results

4.1 Characterization of Particulate matter

Particulate matter (PM-10) include organic and inorganic components named ERM-CZ 100 and ERM-CZ120, purchased from European joint research commission Mainly contain PAH's, Dioxins, PCB's and Zinc, cadmium, mercury, cobalt, SiO2 respectively, particle

size of Particulate matter is less than 10µm and characterized by Scanning electron microscope. Particle size detected in under scanning electron microscopy was less than 10µm Shown in fig. 24a.

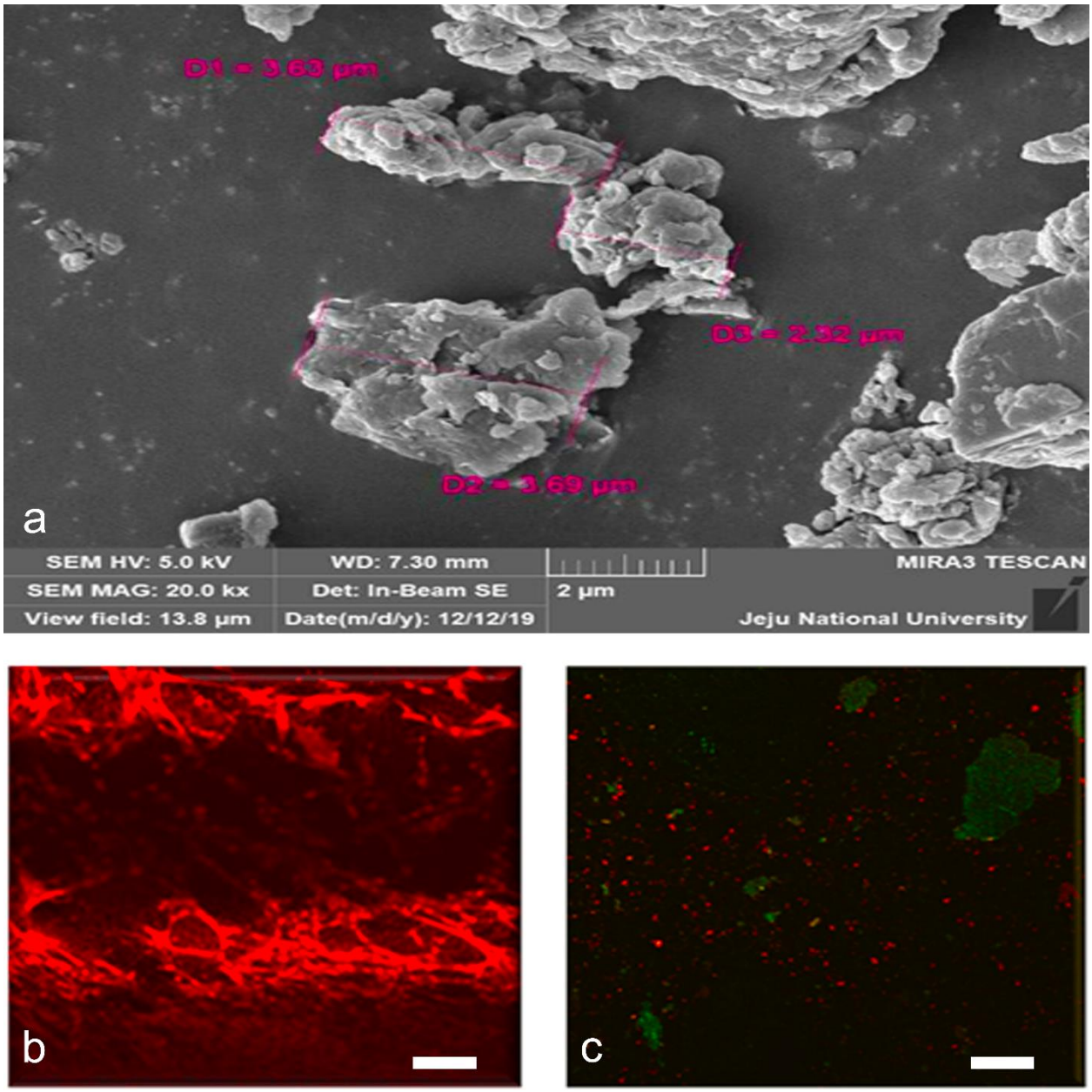

Figure 24. Confocal micrograph of Lung epithelial cells on a microfluidic chip, a). Scanning electron microscope micrograph ERM-CZ-100, ERM-CZ120. Particle size less than 10µm scale bar set at 2µm. showing differentiated epithelium, AT type - I Goblet cells stained with MUC5AC (Green) and AT type-II Ciliated cells stained with Antiß tubulin IV (Red). Scale bar:

100µm b) Epithelial tight junctions, stained with occludin conjugated Alexa flour 594. c) lung on chip showing epithelium, lung small airway and alveolar epithelial cell Goblet with MUC5AC (Green) ciliated cells stained with Antiß tubulin IV (Red). Scale bar: 100µm.

4.2 Impedance data demonstrating barrier integrity:

According to impedance data of our TEER sensor, values in positive control chip started to increase gradually with increasing barrier junctions and increasing confluency of the cells on chip recorded after half an hour interval throughout the experiment. Impedance data demonstrated that the epithelial cells junctions increase with increasing confluency and stable culture for four days at fully confluent monolayer value of impedance was recorded 930Ωcm2 average impedance values in previous studies of lung epithelial cells are 800-980 Ωcm2 Huh et al., 2010. Our lung on chip is providing more accurate data as chip is already printed with ITO based TEER sensor which is directly in contact with cell surface, previously some studies reports TEER values in trans-well culture, embedded sensor approach is first time implemented in a microfluidic platform shown in fig. 25a.

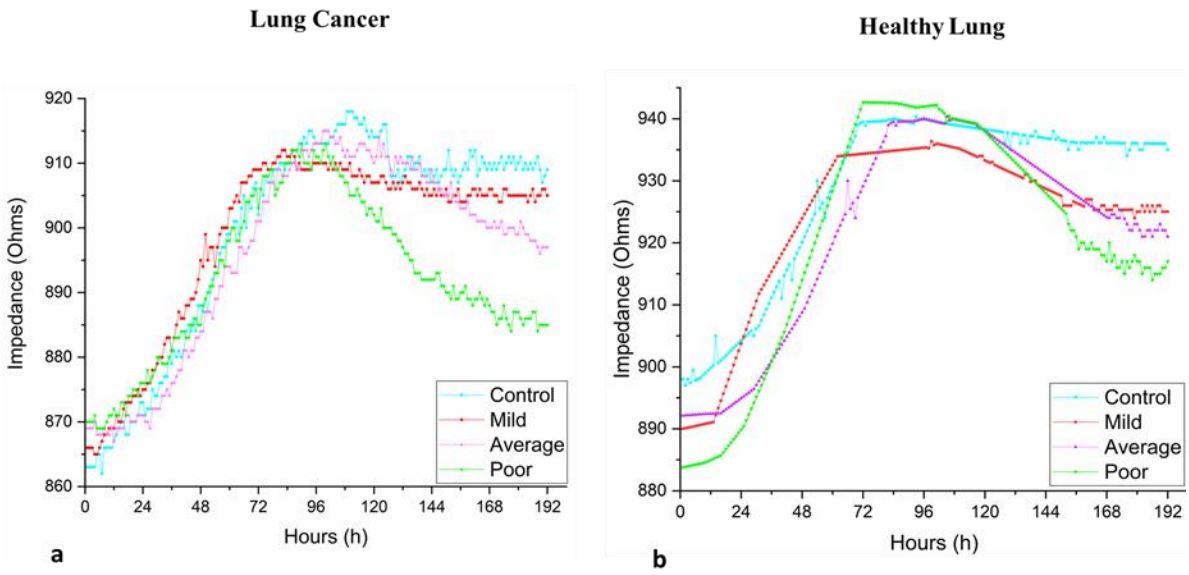

Figure 25. a) Graph representing Impedance values of lung cancer epithelial junctions. Blue line is representing normal chip showing impedance pattern of the complete experiment. Tight junctions' stability achieved on day 3 and red line in representing Particulate matter concentration 7.5µg/ml, showing slight drop in impedance values whereas pink is representing comparatively high concentration of particulate matter 37.5µg/ml. Green line is showing huge drop in impedance values at particulate matter concentration of 151µg/ml. (b) Graph representing Impedance values of healthy lung epithelial junctions. Blue line is representing normal chip showing impedance pattern of the complete experiment. Tight junctions' stability achieved on day 3 and red line in representing Particulate matter concentration 7.5µg/ml, showing slight drop in impedance values whereas pink is representing comparatively high concentration of particulate matter 37.5µg/ml. Green line is showing huge drop in impedance values at particulate matter concentration of 151µg/ml

4.3 Monolayer Membrane integrity epithelium barrier properties

Immunofluorescence analysis by confocal microscopy revealed that this platform has provided ideal growth environment by making complete monolayer of lung epithelial cells and lung cancer monolayer predominantly describing the formation of pseudostratified epithelium with goblet mucus producing and ciliated cells, characterized by epithelial cells marker and morphology specific markers MUC5AC for goblet cells and Antiβ tubulin IV for ciliated cells demonstrated in Fig 3 c. Tight junction's integrity of Lung epithelial cells was evaluated by staining the cells on microfluidic chip with Occludin conjugated Alex flour 594 (Sigma) can be visualize in Fig 3 b. Confocal images provide data that truly complements with impedance values of TEER sensor that complete monolayer integrity and proper morphology of Lung epithelium was achieved in our microfluidic platform.

4.4 Compromised barrier integrity upon particulate matter exposure

Particulate matter exposure at high concentrations significantly disrupts the barrier functions as confocal micrographs are showing in the Fig 26. At relatively low concentration of particulate matter epithelial cell junction marker expressed in control chip but at high concentration of 37.5μg/ml and151μg/ml barrier permeability was lost can be seen in Fig 5 b-d, which was also confirmed by TEER and cytokine analysis measurement. Real time microscope images showing low cell viability in PM treated chips as compared to control chips in (fig 26).

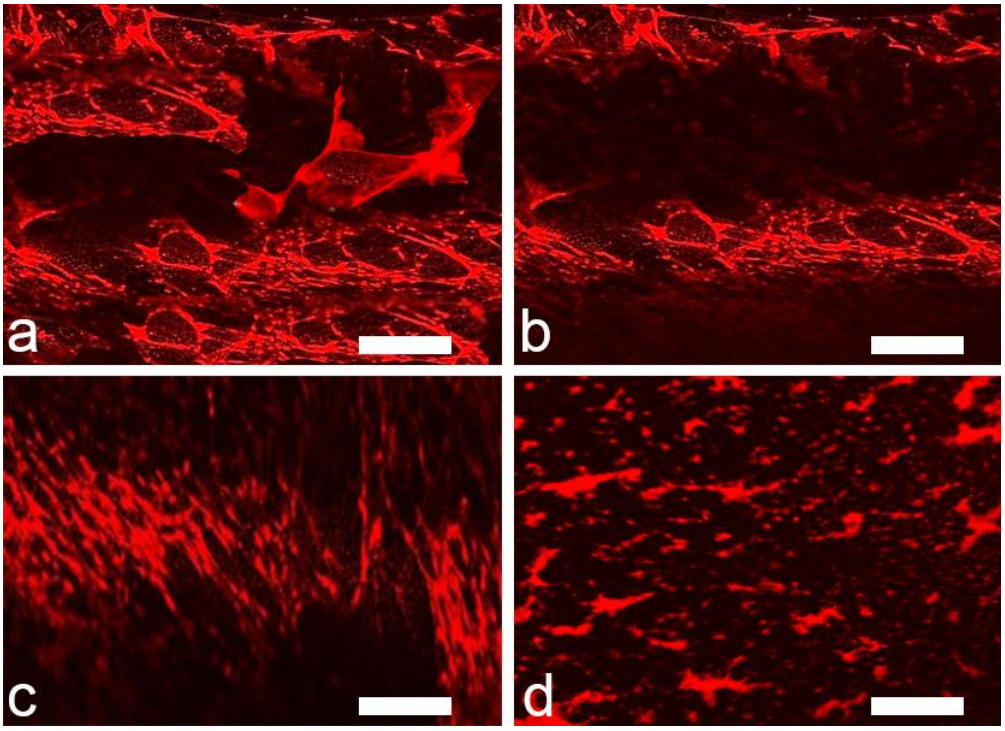

Figure 26. Confocal micrographs of epithelial tight junctions' control and particulate matter treated chips. a) lung epithelial tight junctions stained with Occludin conjugated Alexa flour 594 showing intracellular junctions, b) Particulate matter Treated chip with concentration 7.5µg//ml showing a little compromised integrity. c) Particulate matter treated chip with concentration of 37.5µg//ml showing intracellular barrier damage. d) High concentration of particulate matter treated chip 151µg//ml showing diminishing expression of occludin.

4.5 Confocal imaging of Goblet cell hyperplasia and ciliated cells dysfunction

Polymeric mucin MUC5AC is a low charge glycoform of MUC2 is major secretary protein in patients with chronic respiratory disease asthma, Mucins hypersecretion due to chronic inflammation results in airway diseases such as chronic obstructive pulmonary disease, and cystic fibrosis (CF) [30, 31]. Goblet cell hyperplasia occurs when ciliated cells become unable to maintain airway homeostasis by shutting down mucociliary clearance and macrophage activation and this loss leads to chronic pulmonary disease Fig. 27 b-d.

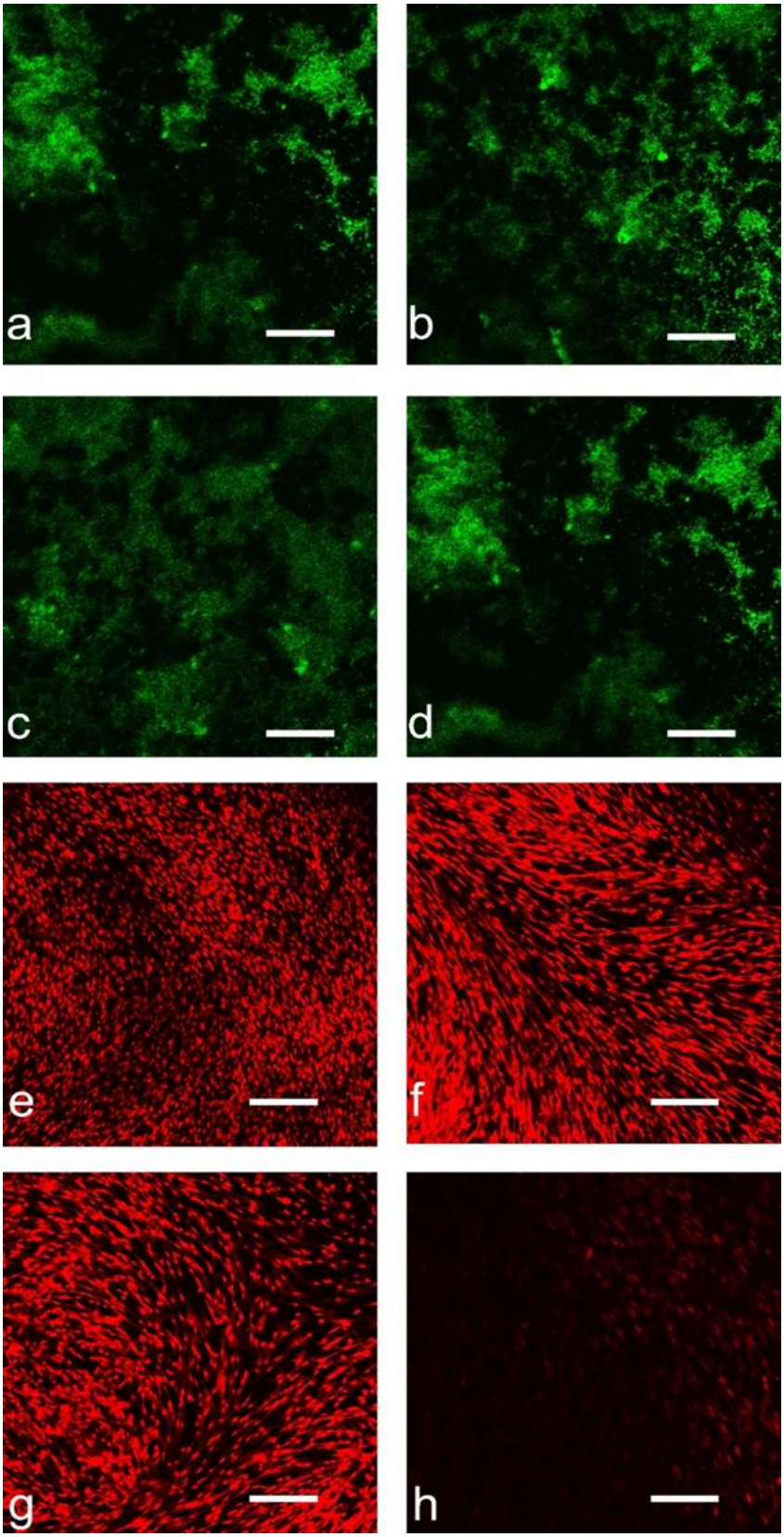

Figure 27. Confocal micrograph of lung epithelial cells exhibiting goblet cell hyperplasia and decreased ciliated cells function in lung on chips after particulate matter exposure. a-d) lung

on chip, human pulmonary epithelium stained with MUC5AC and attached with secondary Alexa flour goat anti mouse-488 Control chip with media showing normal expression of mucin. b) Particulate matter concentration of 7.5µg//ml. showing intensified expression of mucin. c-d) showing high expression of mucin characteristic of asthmatic patients. Scale bar: 100µm

Results demonstrated that expression of mucin (MUC5AC) increased with increasing concentration of particulate matter. High mucin production and loss of mucociliary clearance is rational phenomena. Our results of control and particulate matter treated chips showed a dose dependent increase in mucin production and provide proof of incidence of asthma, COPD and hyperresponsiveness of airway whereas relatively decreased expression of anti-β tubulin IV with increasing concentration of particulate matter which provide proof of loss of mucociliary clearance and decreased cilia beating frequency shown in fig 6 h, which is the most important homeostatic function of distal airway epithelial goblet and ciliated cells shown in Fig 27

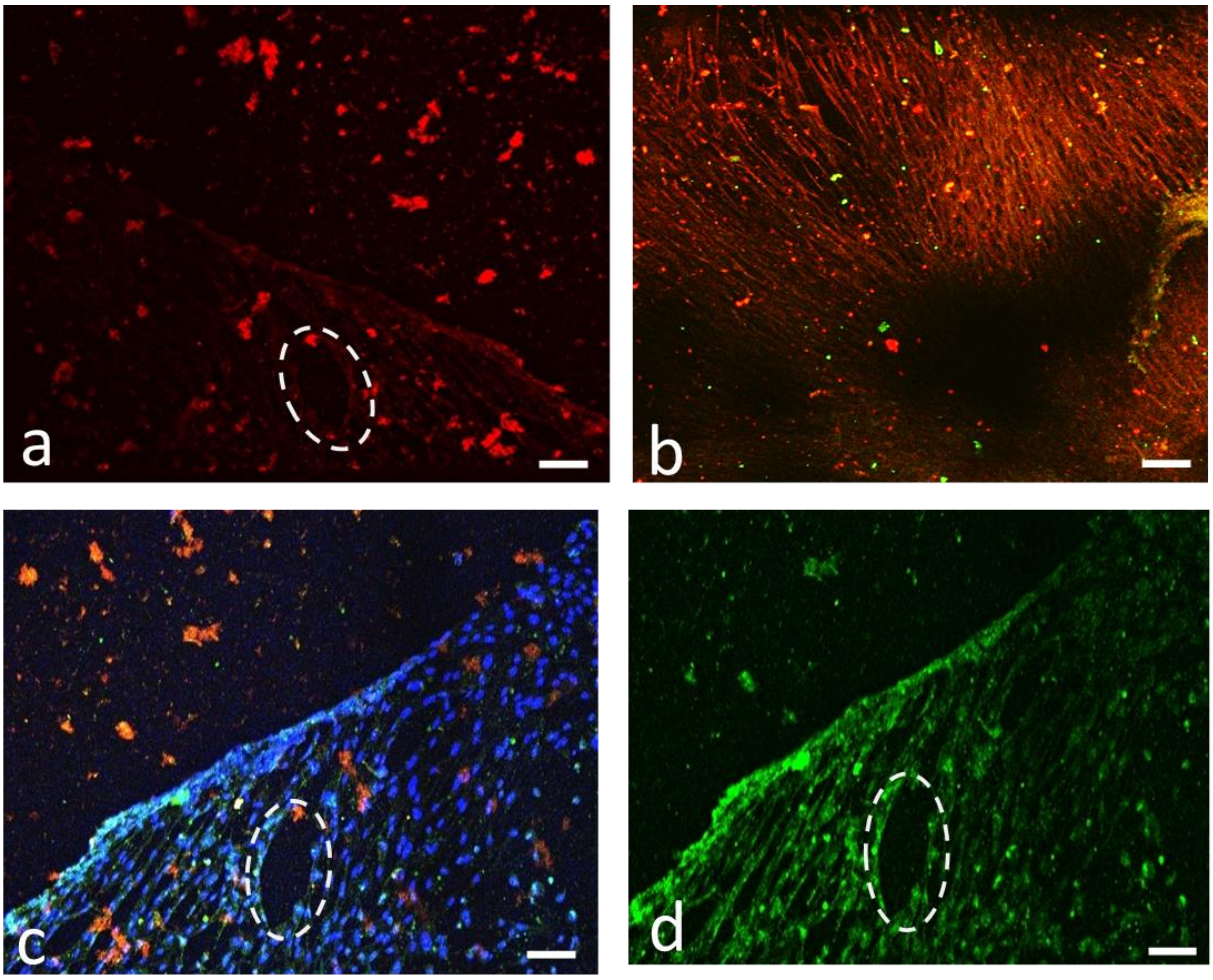

Figure 28 a) Diminishing expression of Anti β Tubulin IV 20X. b) Expression of occludin conjugated Alexa flour 594 merged 20X. c) Mucus hypersecretion as a consequence of high concentration of fine dust 150µg/ml merged counter stained with DAPI at 20X. d) Mucus hypersecretion as a consequence of high concentration of fine dust 150µg/ml stained with MUC5AC antibody and secondary Alexa flour 488 at 20X Scale bar: 100µm

4.6 Confocal imaging of the Cancer invasion in Asthmatic lung

In cancer chips mucus production was high in dose dependent manner in case of mild and average exposures while in poor the expression of MMP-9 was dominating, Even in mild exposure the cell give MMP-9 expression which was increased in average exposure, whereas in case of high concentration of PM mucin expression was less but MMP-9 was providing high expression shown in fig29 a-d.

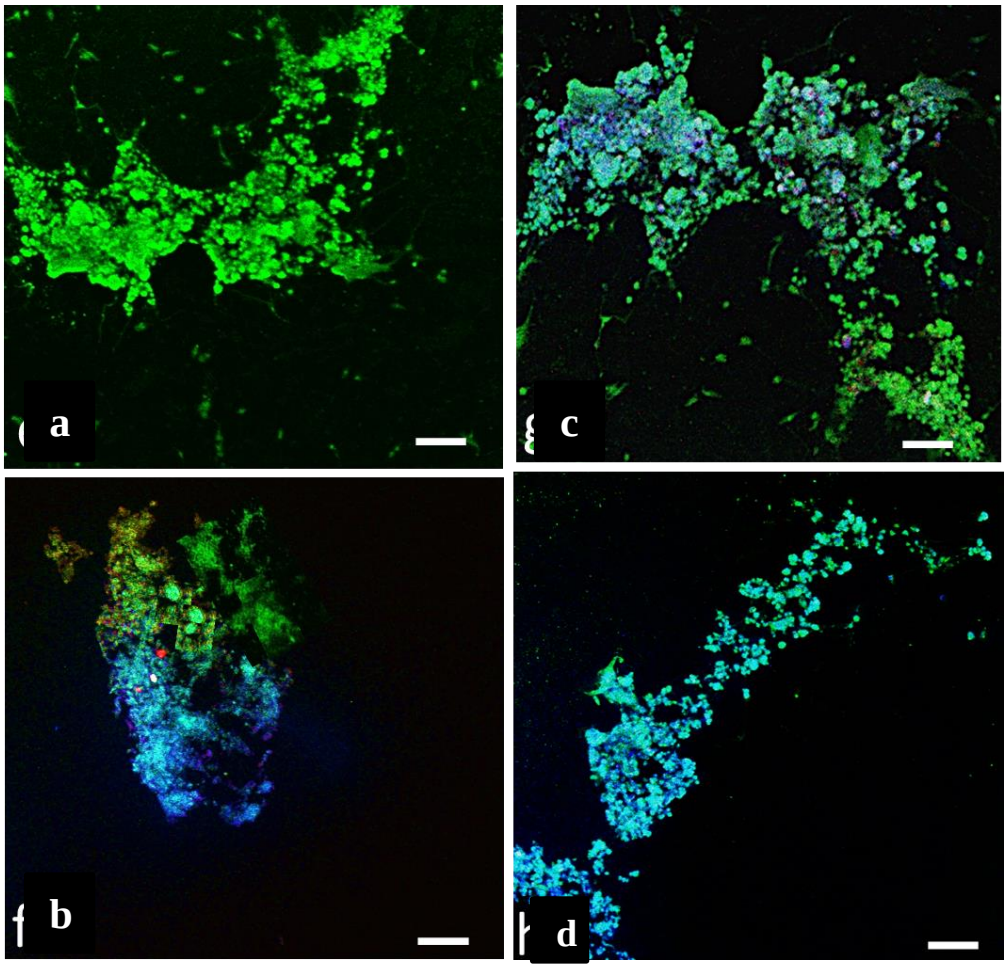

Figure 29 a) Cancer chip representing the control without particulate matter treatment showing only mucin expression. b) Cancer chip treated with PM 7.5µg/ml showing slight magenta color showing little expression of tumor growth and invasion stained with MMP-9 and 30 d secondary Alexa Fluor 647 (magenta). c) Lung cancer chip treated with average

concentration of PM 37.5 µg/ml showing increase in both markers MUC5AC(Green) and MMP9 d) Lung cancer chip treated with poor PM 101.5 µg/ml showing increase in expression of MMP9 whereas decrease in MUC5AC, Scale bar :100µm

4.7 ROS estimation

Cellular injury occurs in lung cells when exposed to particulate matter (PM) [32]. Cr, Co, Ni, Mn, Zn, Cu, and, Fe are the most commonly found elements in airborne PM [33]. Fe is designated as profoundly associated with the manufacture of oxidative stress and enabling superoxide anions (O2 −) and hydrogen peroxide (H2O2) alteration to hydroxyl ions (OH−) [32]. PM exposure results in impaired pulmonary function and surfactant dysfunction [32] inflammatory response leads to damage of epithelial cells, increased vascular permeability. PM includes PAH particularly benzo[a]anthracene, benzo[b] fluoranthene, benzo[k]fluoranthene, and benzo[a] pyrene, are potential carcinogenic risk, in accordance with IARC.

The presence of PAH in PM is related to triggering of inflammation of epithelial and macrophages, ROS generation and lipid peroxidation [34]. In this study DCFDA assay was performed for ROS measurement at the end of the experiment, In control chip healthy alive monolayer of lung epithelial, level of ROS is very low as compared to the particulate matter treated chips and there is a relative increase in the lung epithelial monolayer chips with increasing concentration of particulate matter induced ROS whereas PM treated Cancer chips showed significantly high level of ROS data is presented in the fig 31.

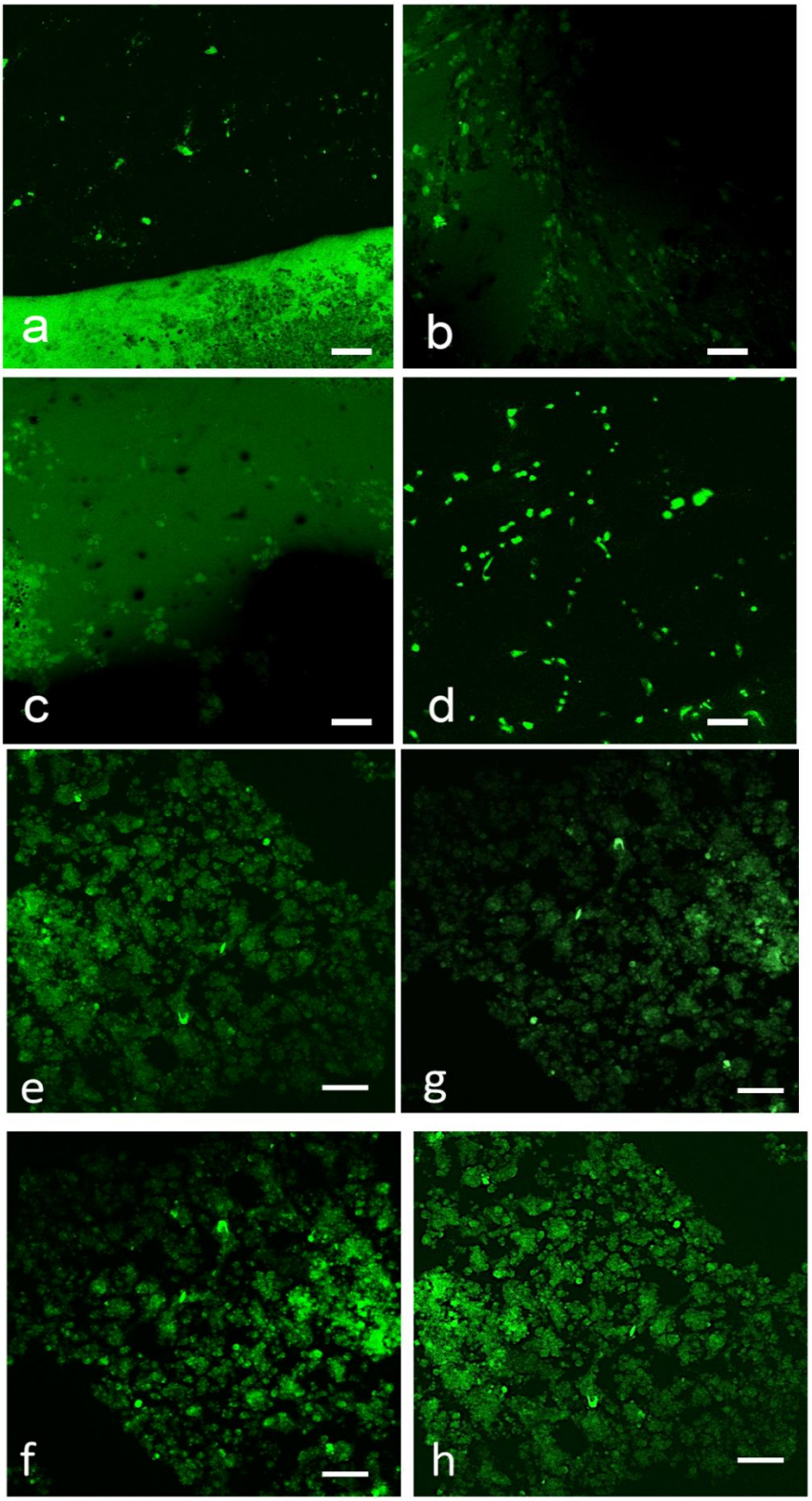

Figure 31Confocal micrographs of DCFDA assay for ROS detection. a) Normal positive control without particulate matter exposure. b) Particulate matter Concentration of 7.5µg//ml

treated lung epithelial cells showing ROS. C-d) Particulate matter concentration 37.5µ //ml, 151µg//ml treated chips respectively showing increased ROS generation in cellular environment. e-h) Cancer chips representing increased ROS generation as compared to normal chips. Scale bar: 100µm

4.8 Cytokine release analysis

IL-13 has a critical role in development of asthma [35]. IL-13 directly affect human airway epithelium and involved in inflammation of respiratory tract, respiratory tract hyperresponsiveness, goblet cell hyperplasia and mucus hypersecretion eventually subepithelial fibrosis occurs as a consequence of airway inflammation similar to that observed in airway mucosa of the individuals with asthma [3637]. In our experiment concentration of IL-13 found highest in media samples at 24 hours after exposure and the maximum concentration was observed in samples of particulate matter concentration 151µg//ml shown in fig 8 c. Whereas, at low particulate matter concentration of 7.5µg/ml interleukin IL-13 concentration was high throughout the experiment. Our data present highly significant values at 24 hour of particulate matter exposure and significant at 72 hours of particulate matter exposure. IL-13 release in cell culture media was analyzed after 12h of particulate matter exposure, bar graph showing significant value at 24h, IL-13 was highest and later on tends to decrease with time until 96h in fig 32b.

IL-13 is associated with various pathological states and also promote the cancer growth and invasion.IL-13 was increased in moderate concentration of particulate matter after 24 hours and increased until 48 hours. IL-6 is a cytokine has been considered as biomarker of inflammation rather than a regulatory cytokine with ability to modulate

immune responses [38]. In response to allergen stimulation to lung airway, IL-6 is released from lung epithelial cells as immune response. Recently IL-6 is involved in adaptive immune response in the differentiation of effector CD4+T cells, Particularly it has function in suppressing Th1 and thus induce TH-2 differentiation of CD4+T cells via independent cytokine regulatory pathways . Many studies have provided the data for generation of IL-16 in combination with TGF- β for promotion of murine Th17 cells where as some studies relate it with IL-1β to promote Th-17 [31].

Interleukin-6 showed damage dependent release from lung epithelial cells, IL-6 in media samples increased with time at higher concentration of damage inducing stimulus particulate matter. Maximum concentration of particulate matter was detected after three days of exposure and later it tends to decrease. Pattern of cytokines release in our Lung epithelial cell provide the significant data about inflammation of cells by particulate matter stress in acute conditions at 24 and 48 hours after exposure shown in fig 8 a. In lung cancer IL-6 promote tumor growth and progression, IL-6 increase in serum was measured after exposure of particulate matter after 48 hours IL-6 was significantly high after 72 hours IL-6 was still increasing. In cancer chip 2 folds increase was measured in fig 32d. TNF-α is a cytokine and well-studied biomarker of PM stressed conditions in human and secreted as immune response, it is secreted by epithelial cells after ROS generation in mitochondria and leads to NF-Kappa-B pathway. TNF-α concentration was measured highest on increasing stress signal graph showed that concentration of this cytokine increased only at high concentration of particulate matter exposure, whereas lower concentration release of TNF-α is comparatively low this data presented significant value of the concentration after 24

and 72 hours of particulate matter exposure, In case of Cancer chips trend was increased two three folds shown in fig. 32e [39].

Mucin is a secretory glycoprotein which is a potential biomarker observed in bronchioalveolar lavage and sputum samples of asthmatic patients, Mucin levels gradually increase in particulate matter treated chips with increasing concentration of particulate matter. Mucin release in cell culture media was also noted as dose and time dependent because highly oxidative environment is the cause of bronchoconstriction and decreased mucociliary clearance. After 2 days of particulate matter exposure at high concentration leads to release of 400pg/ml mucin fig 32c. All the cytokines showed significant increase in the concentration of cancer chips in fig 32 e-h.

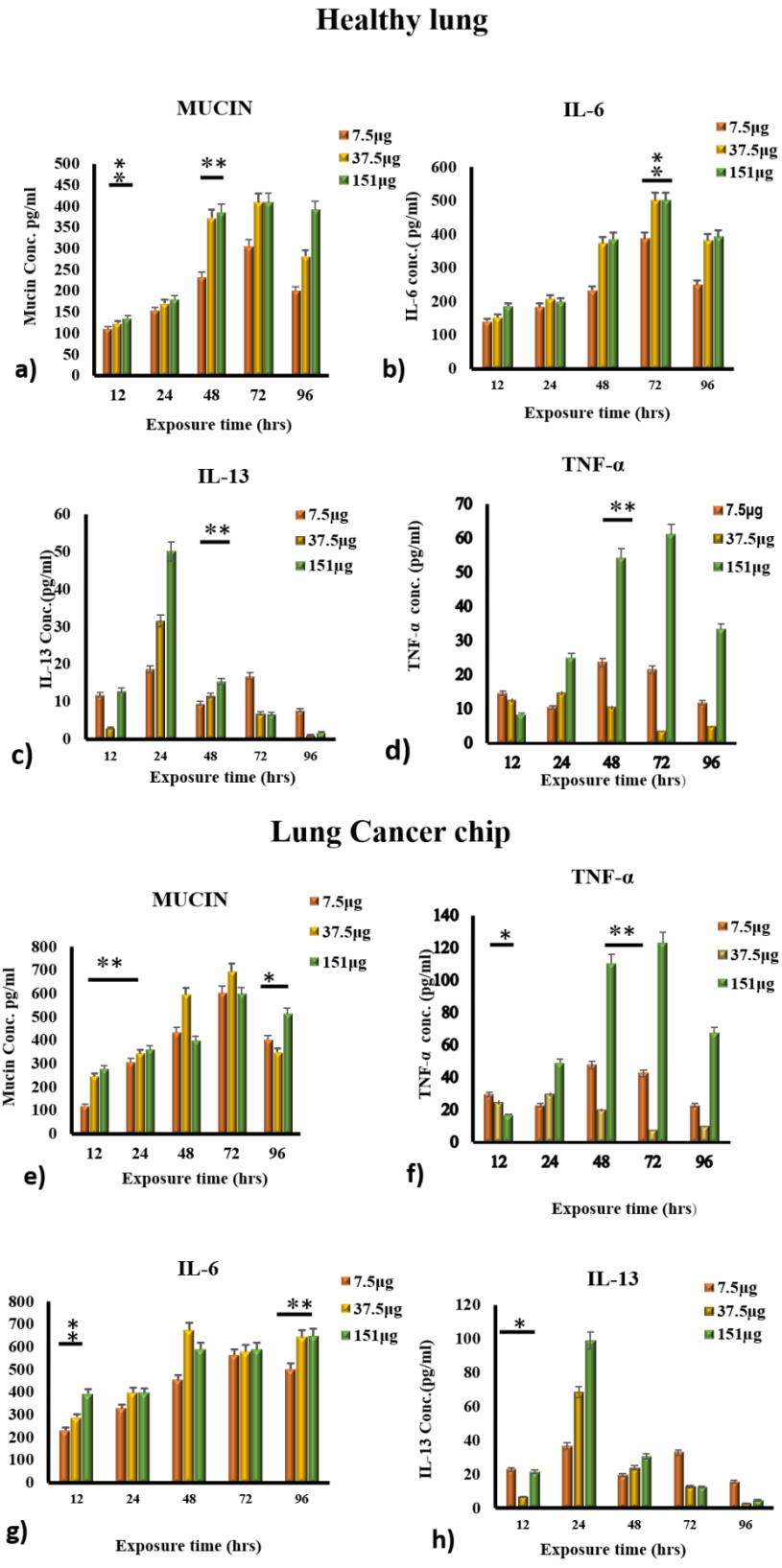

Figure 32 Graphs representing cytokines concentrations in pg./ml on X-axis and exposure time at y-axis. a) Mucin release in cell culture media was also noted as dose and time

dependent because highly oxidative environment is the cause of bronchoconstriction and de creased muco-ciliary clearance. After 2 days of particulate matter exposure at high concentration leads to release of 400pg/ml mucin. Significance was calculated by P-value. Presented in data (P<0.05) as (*) and highly significant value presented as (P<0.001) b) IL-6 concentration in cell culture media was recorded at 12, 24, 48 ,72 and 96 hours, IL-6 concentration started increasing after 24h and in Correlation to ROS production its concentration was high at 96 hours till end of the experiment. c) (**).IL-13 release in cell culture media was analyzed after 12h of particulate matter exposure, bar graph showing significant value at 24h, IL-13 was highest and later on tends to decreased with time until 96h. Significance was calculated by P-value. Presented in data (P<0.05) as (*) and highly significant value presented as (P<0.001) (**). d) Graph representing cytokines concentrations in pg./ml on X-axis with respect to exposure time at y-axis. Concentration of TNF-α showed dose dependent pattern of cytokine release with respect to the stimulant particulate matter exposure at low concentration TNF-α concentration in cell culture media is around 30pg/ml whereas at high concentration of particulate matter exposure release of cytokine was maximum at after 3 days of exposure. e) Mucin release in cell culture media was also noted as dose and time dependent because highly oxidative environment is the cause of bronchoconstriction and decreased mucociliary clearance. After 2 days of particulate matter exposure at high concentration leads to release of 400pg/ml mucin. Significance was calculated by P-value. Presented in data (P<0.05) as (*) and highly significant value presented as (P<0.001). f. Graph representing cytokines concentrations in pg./ml on X-axis with respect to exposure time at y-axis. Concentration of TNF-α showed dose dependent pattern of cytokine release with respect to the stimulant particulate matter exposure at low concentration TNF-α concentration in cell culture media is around 30pg/ml whereas at high

concentration of particulate matter exposure release of cytokine was maximum at after 3 days of exposure. g) IL-6 concentration in cell culture media was recorded at 12, 24, 48 ,72 and 96 hours, IL-6 concentration started increasing after 24h and in Correlation to ROS production its concentration was high at 96 hours till end of the experiment. h) IL-13 release in cell culture media was analyzed after 12h of particulate matter exposure, bar graph showing significant value at 24h, IL-13 was highest and later on tends to decreased with time until 96h. Significance was calculated by P-value. Presented in data (P<0.05) as (*) and highly significant value presented as (P<0.001) (**).

5. Discussion

Here in this study, we have established an efficient and robust organ on chip system for mechanical, chemical, and environmental toxicological analysis. Our organ on chip system is unique owing to its capacity to address previously reported limitations of the organs on chip we have introduced a reconfigurable glass based chip with transparent printed TEER electrode, sensor embedded in the system and real time microscope for real time analysis of different environmental conditions, PM pollution around the globe is responsible for causing fatal respiratory diseases i.e., asthma, COPD, and [40]interstitial lung disease. Lack of appropriate models to study such real time conditions results in failure of effective and prompt drug development for the treatment of these harmful diseases, In past many studies have introduced their organ on chip devices for recapitulating real time phenomenon nevertheless there have been limitation such as embedded sensor and PDMS based chips. In current attempt we're introducing our model with monolayer primary cell

culture on chip, is an initial validation of our platform, sensors and microscope. We have tried to recapitulate environmental condition PM induced possible diseased conditions which is validated by presence of cytokines IL-13, TNF-α, IL-6 and mucin.

To achieve this goal, we select three levels of PM provided by daily climate control conditions of the country, Good, bad and worst and followed the exposure scheme that one individual can experience in a week. First, we characterized our monolayer chip permeability by TEER and confocal microscopy. Later we introduced PM stimulus to induce diseased conditions in our chip with three different concentrations for 4 days of daily exposure of 8 hours. For toxicity analysis media samples were collected from 12 hours after first treatment and then after every 24 hours, Impedance values were providing every change in the permeability of epithelium right after every half an hour. TEER, microscope results were recorded automatically by software installed in computer attached to the organ on chip system.

Data from TEER software demonstrate that barrier permeability increased up to 80% for first four days in all chips, whereas in PM treated chips barrier permeability was started compromising after 12 hours of exposure, Cytokines analysis of the selected biomarkers followed the regular pattern of increasing toxicity in a dose dependent manner.

Immunofluorescence analysis of the control and PM treated chips provide proof of normal and diseased conditions. Expression of Occludin for permeability of tights junctions in control chips and in PM treated chip showed huge difference and pointed out the inflammatory conditions and morphology specific biomarkers such as Mucin and anti-β tubulin IV give the whole picture of the experiment. Mucin enriched lung epithelium is a known characteristic of asthmatic patients and because ciliated cells functions halt due and

mucociliary movements almost shuts down because of pulmonary stress in cancer patients this condition aggravates complications and hyperresponsiveness. IL-13 is the cytokines which promotes the mucin production by increasing eosinophils recruitment, in our ELISA for IL-13 PM induce increased production of this cytokine after 24 hours and the IL-13 release was significantly high in worst conditions of particulate matter.

Release of mucin is linked to IL-13, Increase in concentration of mucin release from lung epithelial cells is a proof of defective function of the ciliated cells which are involved in the mucociliary clearance Mucin ELISA graph is augmenting the confocal micrographs and validate our platform for recapitulating human physiology at alveolar level by showing increasing concentration of mucin at high concentrations of particulate matter and for long time exposure, such biomarker could provide incidence of many diseases in our automated and sophisticated organ on chip platforming cancer chips mucin level was also increased . IL-6 is a proinflammatory cytokine produced in asthma and COPD conditions and is related to acute impaired lung function[41]. In our data IL-6 concentration showed gradual increase in the production of this cytokines and this is associated with evidence of asthma patients sputum samples as published by a study [42]. IL-6 secretion was increased two folds in cancer chips treated with PM. TNF- α is expressed by increasing ROS production in airway epithelium and lung cancer epithelium respectively[43], Oxidative stress and free radical production occurs as inflammatory response of associated to PM exposure reported previously in many studies[44].Several evidences have provided information of validity of our platform for successful toxicological analysis and reconstituting organ pathophysiology, future target of our group is to study the complex tissue physiology with integration of embedded sensors. Graph representing mucin levels in fig 8 c showing increase in mucin

release in supernatant is also comparable with confocal micrographs. In future, this device will help to design complex tissue mimetics of human physiology and disease model for toxicity testing.

Conclusion

Technological advancements in organ on chip technology are offering robust and efficient solutions for drug discovery and therapeutic evaluation. Our microfluidic lung on chip and lung cancer on chip devices has potential to mimic normal and diseased human physiology as well as environmental and pathological conditions. According to the results obtained from this study, we have validated that this well-equipped system with reconfigurable microchip, portable microscope for Real time monitoring of cells, system integrated TEER sensor would help in the development of better human physiological and pathological mimetics. High metabolic activity of the lung epithelial cells tumor growth was analyzed in this dynamic fluid flow environment as compared to the static culture conditions. High levels of cytokines were observed in this device due to optimized recirculation media conditions in both types of disease models. The primary challenge of building an organ on chip is to duplicate *in vivo* environment for housing an organ with ease of handling and robustness. Second challenge of organ on chip technology is manufacturing of cost effective, toxicity evaluation with help of system embedded sensor. This device has provided the preliminary data for making this breakthrough in OOC technology. Future perspective of our group is to make complex tissue mimetics of human for toxicity testing and drug discovery with system integrated pathological sensors for replacing time consuming molecular analysis of pathological conditions.

Declaration

I (Faiza Jabbar), hereby declare that this thesis entitled "**Development of lung on a chip for mimicking particulate matter exposure conditions**", submitted to Jeju National University in the partial fulfillment of the requirements for the award of the **Degree of Doctor of Philosophy** in the department **of Mechatronics Engineering** is a record of original and independent research work done and published by during the period March 2018 to February 2021 under the supervision of the **Professor Kyung Hyung Choi.** This thesis work is based on the publications in reputed journals and it has not been formed for the award of any other Degree/Diploma/Associateship/Fellowship to any individual of any university.

Faiza Jabbar

References

(1) Deng, J.; Qu, Y.; Liu, T.; Jing, B.; Zhang, X.; Chen, Z.; Luo, Y.; Zhao, W.; Lu, Y.; Lin, B. Recent Organ-on-a-Chip Advances toward Drug Toxicity Testing. *Microphysiological Syst.* **2018**, *1*, 1–1. https://doi.org/10.21037/mps.2018.09.02.

(2) Lee, Y. G.; Ho, C. H.; Kim, J. H.; Kim, J. Quiescence of Asian Dust Events in South Korea and Japan during 2012 Spring: Dust Outbreaks and Transports. *Atmos. Environ.* **2015**, *114*, 92–101. https://doi.org/10.1016/j.atmosenv.2015.05.035.

(3) Lelieveld, J.; Evans, J. S.; Fnais, M.; Giannadaki, D.; Pozzer, A. The Contribution of Outdoor Air Pollution Sources to Premature Mortality on a Global Scale. *Nature* **2015**, *525* (7569), 367–371. https://doi.org/10.1038/nature15371.

(4) Gilmour, M. I.; Daniels, M.; McCrillis, R. C.; Winsett, D.; Selgrade, M. K. Air Pollutant-Enhanced Respiratory Disease in Experimental Animals. *Environ. Health Perspect.* **2001**, *109* (August), 619. https://doi.org/10.2307/3454680.

(5) Becker, S.; Mundandhara, S.; Devlin, R. B.; Madden, M. Regulation of Cytokine Production in Human Alveolar Macrophages and Airway Epithelial Cells in Response to Ambient Air Pollution Particles: Further Mechanistic Studies. *Toxicol. Appl. Pharmacol.* **2005**, *207* (2 SUPPL.), 269–275. https://doi.org/10.1016/j.taap.2005.01.023.

(6) Martignoni, M.; Groothuis, G. M. M.; de Kanter, R. Species Differences between Mouse, Rat, Dog, Monkey and Human CYP-Mediated Drug Metabolism, Inhibition and Induction. *Expert Opin. Drug Metab. Toxicol.* **2006**, *2* (6), 875–894. https://doi.org/10.1517/17425255.2.6.875.

(7) Whitesides, G. M.; Ostuni, E.; Jiang, X.; Ingber, D. E. S Oft L Ithography in B Iology. *Annu. Rev. Biomed. Eng.* **2001**, *3*, 335–373.

(8) Miyata, R.; Hiraiwa, K.; Cheng, J. C.; Bai, N.; Vincent, R.; Francis, G. A.; Sin, D. D.; Van Eeden, S. F. Statins Attenuate the Development of Atherosclerosis and Endothelial Dysfunction Induced by Exposure to Urban Particulate Matter (PM10). *Toxicol. Appl. Pharmacol.* **2013**, *272* (1), 1–11. https://doi.org/10.1016/j.taap.2013.05.033.

(9) Erickson, D.; Li, D. Integrated Microfluidic Devices. *Anal. Chim. Acta* **2004**, *507* (1), 11–26. https://doi.org/10.1016/j.aca.2003.09.019.

(10) Odijk, M.; Van Der Meer, A. D.; Levner, D.; Kim, H. J.; Van Der Helm, M. W.; Segerink, L. I.; Frimat, J. P.; Hamilton, G. A.; Ingber, D. E.; Van Den Berg, A. Measuring Direct Current Trans-Epithelial Electrical Resistance in Organ-on-a-Chip Microsystems. *Lab Chip* **2015**, *15* (3), 745–752. https://doi.org/10.1039/c4lc01219d.

(11) Soomro, A. M.; Jabbar, F.; Ali, M.; Lee, J. W.; Mun, S. W.; Choi, K. H. All-Range Flexible and Biocompatible Humidity Sensor Based on Poly Lactic Glycolic Acid (PLGA) and Its Application in Human Breathing for Wearable Health Monitoring. *J. Mater. Sci. Mater. Electron.* **2019**, *30* (10), 9455–9465. https://doi.org/10.1007/s10854-019-01277-1.

(12) Khalid, M. A. U.; Kim, Y. S.; Ali, M.; Lee, B. G.; Cho, Y. J.; Choi, K. H. A Lung Cancer-on-Chip Platform with Integrated Biosensors for Physiological Monitoring and Toxicity Assessment. *Biochem. Eng. J.* **2020**, *155* (September 2019), 107469. https://doi.org/10.1016/j.bej.2019.107469.

(13) Reardon, S. "Organs-on-Chips" Go Mainstream. *Nature* **2015**, *523* (7560), 266. https://doi.org/10.1038/523266a.

(14) Squires2005.Pdf.

(15) Haeberle, S.; Zengerle, R. Microfluidic Platforms for Lab-on-a-Chip Applications. *Lab Chip* **2007**, *7* (9), 1094–1110. https://doi.org/10.1039/b706364b.

(16) Kwon, J. S.; Oh, J. H. Microfluidic Technology for Cell Manipulation. *Appl. Sci.* **2018**, *8* (6). https://doi.org/10.3390/app8060992.

(17) Wu, Q.; Liu, J.; Wang, X.; Feng, L.; Wu, J.; Zhu, X.; Wen, W.; Gong, X. Organ-on-a-Chip: Recent Breakthroughs and Future Prospects. *Biomed. Eng. Online* **2020**, *19* (1), 1–19. https://doi.org/10.1186/s12938-020-0752-0.

(18) Ben-David, U.; Ha, G.; Tseng, Y. Y.; Greenwald, N. F.; Oh, C.; Shih, J.; McFarland, J. M.; Wong, B.; Boehm, J. S.; Beroukhim, R.; Golub, T. R. Patient-Derived Xenografts Undergo Mouse-Specific Tumor Evolution. *Nat. Genet.* **2017**, *49* (11), 1567–1575. https://doi.org/10.1038/ng.3967.

(19) Zhang, B.; Korolj, A.; Lai, B. F. L.; Radisic, M. Advances in Organ-on-a-Chip Engineering. *Nat. Rev. Mater.* **2018**, *3* (8), 257–278. https://doi.org/10.1038/s41578-018-0034-7.

(20) Xie, Y.; Zhi, X.; Su, H.; Wang, K.; Yan, Z.; He, N.; Zhang, J.; Chen, D.; Cui, D. A Novel Electrochemical Microfluidic Chip Combined with Multiple Biomarkers for Early Diagnosis of Gastric Cancer. *Nanoscale Res. Lett.* **2015**, *10* (1), 1–9. https://doi.org/10.1186/s11671-015-1153-3.

(21) Lind2016.Pdf.

(22) Henry2017.Pdf.

(23) Huh, D.; Matthews, B. D.; Mammoto, A.; Montoya-Zavala, M.; Yuan Hsin, H.; Ingber, D. E. Reconstituting Organ-Level Lung Functions on a Chip. *Science (80-.).* **2010**, *328* (5986), 1662–1668. https://doi.org/10.1126/science.1188302.

(24) Huh, D.; Leslie, D. C.; Matthews, B. D.; Fraser, J. P.; Jurek, S.; Hamilton, G. A.; Thorneloe, K. S.; McAlexander, M. A.; Ingber, D. E. A Human Disease Model of Drug Toxicity-Induced Pulmonary Edema in a Lung-on-a-Chip Microdevice. *Sci. Transl. Med.* **2012**, *4* (159). https://doi.org/10.1126/scitranslmed.3004249.

(25) Bhatia, S. N.; Balis, U. J.; Yarmush, M. L.; Toner, M. Effect of Cell–Cell Interactions in Preservation of Cellular Phenotype: Cocultivation of Hepatocytes and Nonparenchymal Cells. *FASEB J.* **1999**, *13* (14), 1883–1900. https://doi.org/10.1096/fasebj.13.14.1883.

(26) Jang, K. J.; Suh, K. Y. A Multi-Layer Microfluidic Device for Efficient Culture and Analysis of Renal Tubular Cells. *Lab Chip* **2010**, *10* (1), 36–42. https://doi.org/10.1039/b907515a.

(27) Oberdörster, G.; Oberdörster, E.; Oberdörster, J. Nanotoxicology: An Emerging Discipline Evolving from Studies of Ultrafine Particles. *Environ. Health Perspect.* **2005**, *113* (7), 823–839. https://doi.org/10.1289/ehp.7339.

(28) Klein, S. G.; Serchi, T.; Hoffmann, L.; Blömeke, B.; Gutleb, A. C. An Improved 3D Tetraculture System Mimicking the Cellular Organisation at the Alveolar Barrier to Study the Potential Toxic Effects of Particles on the Lung. *Part. Fibre Toxicol.* **2013**, *10* (1). https://doi.org/10.1186/1743-8977-10-31.

(29) Xu, C.; Zhang, M.; Chen, W.; Jiang, L.; Chen, C.; Qin, J. Assessment of Air Pollutant PM2.5 Pulmonary Exposure Using a 3D Lung-on-Chip Model. *ACS Biomater. Sci. Eng.* **2020**, *6* (5), 3081–3090. https://doi.org/10.1021/acsbiomaterials.0c00221.

(30) Marini, M.; Vittori, E.; Hollemborg, J.; Mattoli, S. Expression of the Potent Inflammatory Cytokines, Granulocyte-Macrophage-Colony-Stimulating Factor and Interleukin-6 and Interleukin-8, in Bronchial Epithelial Cells of Patients with Asthma. *J. Allergy Clin. Immunol.* **1992**, *89* (5), 1001–1009. https://doi.org/10.1016/0091-6749(92)90223-O.

(31) Kicic, A.; Sutanto, E. N.; Stevens, P. T.; Knight, D. A.; Stick, S. M. Intrinsic Biochemical and Functional Differences in Bronchial Epithelial Cells of Children with Asthma. *Am. J. Respir. Crit. Care Med.* **2006**, *174* (10), 1110–1118. https://doi.org/10.1164/rccm.200603-392OC.

(32) Lee, H. J.; Ryu, J.; Park, S. H.; Seo, E. K.; Han, A. R.; Lee, S. K.; Kim, Y. S.; Hong, J. H.; Seok, J. H.; Lee, C. J. Suppressive Effects of Coixol, Glyceryl Trilinoleate and Natural Products Derived from Coix Lachryma-Jobi Var. Ma-Yuen on Gene Expression, Production and Secretion of Airway MUC5AC Mucin. *Arch. Pharm. Res.* **2015**, *38* (5), 620–627. https://doi.org/10.1007/s12272-014-0377-6.

(33) Morcillo, E. J.; Cortijo, J. Mucus and MUC in Asthma. *Curr. Opin. Pulm. Med.* **2006**, *12* (1), 1–6. https://doi.org/10.1097/01.mcp.0000198064.27586.37.

(34) Stohs, S. J.; Bagchi, D. Oxidative Mechanisms in the Toxicity of Metal Ions. *Free Radic. Biol. Med.* **1995**, *18* (2), 321–336. https://doi.org/10.1016/0891-5849(94)00159-H.

(35) Chauhan, S. S.; Misra, U. K. Elevation of Rat Pulmonary, Hepatic and Lung Surfactant Lipids by Fly Ash Inhalation. *Biochem. Pharmacol.* **1991**, *41* (2), 191–198. https://doi.org/10.1016/0006-2952(91)90476-L.

(36) Castaño-Vinyals, G.; D'Errico, A.; Malats, N.; Kogevinas, M. Biomarkers of Exposure to Polycyclic Aromatic Hydrocarbons from Environmental Air Pollution. *Occup. Environ. Med.* **2004**, *61* (4), 1–10. https://doi.org/10.1136/oem.2003.008375.

(37) Thomsen, A. E.; Friedrichsen, G. M.; Sørensen, A. H.; Andersen, R.; Nielsen, C. U.; Brodin, B.; Begtrup, M.; Frokjaer, S.; Steffansen, B. Prodrugs of Purine and Pyrimidine Analogues for the Intestinal Di/Tri-Peptide Transporter PepT1: Affinity for HPepT1 in Caco-2 Cells, Drug Release in Aqueous Media and in Vitro Metabolism. *J. Control. Release* **2003**, *86* (2–3), 279–292. https://doi.org/10.1016/S0168-3659(02)00413-3.

(38) Martinez-Nunez, R. T.; Louafi, F.; Sanchez-Elsner, T. The Interleukin 13 (IL-13) Pathway in Human Macrophages Is Modulated by MicroRNA-155 via Direct Targeting of Interleukin 13 Receptor A1 (IL13Rα1). *J. Biol. Chem.* **2011**, *286* (3), 1786–1794.

https://doi.org/10.1074/jbc.M110.169367.

(39) Kamimura, D.; Ishihara, K.; Hirano, T. IL-6 Signal Transduction and Its Physiological Roles: The Signal Orchestration Model. *Rev. Physiol. Biochem. Pharmacol.* **2003**, *149*, 1–38. https://doi.org/10.1007/s10254-003-0012-2.

(40) Dienz, O.; Rincon, M. The Effects of IL-6 on CD4 T Cell Responses. *Clin. Immunol.* **2009**, *130* (1), 27–33. https://doi.org/10.1016/j.clim.2008.08.018.

(41) Bettelli, E.; Carrier, Y.; Gao, W.; Korn, T.; Strom, T. B.; Oukka, M.; Weiner, H. L.; Kuchroo, V. K. Reciprocal Developmental Pathways for the Generation of Pathogenic Effector TH17 and Regulatory T Cells. *Nature* **2006**, *441* (7090), 235–238. https://doi.org/10.1038/nature04753.

(42) Acosta-Rodriguez, E. V.; Napolitani, G.; Lanzavecchia, A.; Sallusto, F. Interleukins 1β and 6 but Not Transforming Growth Factor-β Are Essential for the Differentiation of Interleukin 17-Producing Human T Helper Cells. *Nat. Immunol.* **2007**, *8* (9), 942–949. https://doi.org/10.1038/ni1496.

(43) Benam, K. H.; Novak, R.; Nawroth, J.; Hirano-Kobayashi, M.; Ferrante, T. C.; Choe, Y.; Prantil-Baun, R.; Weaver, J. C.; Bahinski, A.; Parker, K. K.; Ingber, D. E. Matched-Comparative Modeling of Normal and Diseased Human Airway Responses Using a Microengineered Breathing Lung Chip. *Cell Syst.* **2016**, *3* (5), 456-466.e4. https://doi.org/10.1016/j.cels.2016.10.003.

(44) Grubek-Jaworska, H.; Paplińska, M.; Hermanowicz-Salamon, J.; Biaek-Gosk, K.; Dbrowska, M.; Grabczak, E.; Domagaa-Kulawik, J.; Stpień, J.; Chazan, R. IL-6 and IL-13 in Induced Sputum of COPD and Asthma Patients: Correlation with Respiratory Tests. *Respiration* **2012**, *84* (2), 101–107. https://doi.org/10.1159/000334900.